BABAR Analysis Document #144, Version 8
May 24, 2001

Measurements of the charged and neutral B meson lifetimes using fully reconstructed B decays [1]

Abstract

Fully reconstructed hadronic B decays are used to measure the lifetimes of both charged and neutral B mesons, as well as their ratio. This analysis is based on the Run1 dataset.

[1]Direct contributors to this document are: Jacques Chauveau (Paris), Fernando Martinez-Vidal (Pisa), Jan Stark (primary editor, Paris).

Contents

1 Introduction

We measure the $B^{\pm}$ and $B^0/\overline{B}^0$ lifetimes as well as their ratio using events that contain one fully reconstructed B candidate. The data sample consists of 20.7 fb^{-1} of e^+e^- collisions collected near the $\Upsilon(4S)$ by the *BABAR* detector in 1999 and in 2000.

We fully reconstruct clean hadronic two-body decay modes to hidden and open charm. Full reconstruction of the B mesons benefits from powerful constraints that can be used to distinguish charged Bs from neutral Bs. The individual lifetimes of the two species can be measured separately, rather than an average "B lifetime".

An inclusive technique is used to reconstruct the decay vertex of the second B in an event, and the lifetimes are determined from the distance between the decay vertices of the two B mesons. This novel method, developed for use at an asymmetric B Factory, deals with event topologies similar to those in measurements of time-dependent *CP* asymmetries. In the latter analyses, the distance between the two decay vertices is used to follow the time-dependence. The measurement of B lifetimes using this novel technique is a significant step towards *CP* violation analyses.

The simple spectator quark decay model predicts equal lifetimes for charged and neutral B mesons. Differences in the lifetimes can arise, e.g. from non-spectator effects like weak annihilation and W exchange. As the b quark is significantly heavier than the c quark, the expected difference of the two B meson lifetimes is much smaller than that observed for their charmed counterparts ($\tau_{D^+}/\tau_{D^0} \simeq 2.5$ [1]). Various models, e.g. [2, 3], give different predictions for a lifetime difference of up to 20 %. At present, the world averages for the B lifetimes and their ratio are [1]: τ_0=1.548±0.032 ps; τ_-=1.653±0.028 ps; τ_-/τ_0=1.062±0.029. These numbers are the combined results from several experiments at SLD, LEP and CDF. The precision is not yet sufficient to make a meaningful distinction between different models. The *BABAR* experiment has reached an interesting level of precision for results obtained with a different method and different systematic errors.

The method used to determine the B meson lifetimes is outlined in section 2. The Run1 dataset and the detector components most relevant to this measurement are reviewed in section 3. B reconstruction and the signal yields are described next (section 4). The measurements of the decay vertices of the two B mesons in each selected event are discussed in section 5. Studies of the resolution on the distance between the two vertices are presented. A thorough understanding of this resolution is necessary to disentangle the effects of the B lifetimes and the detector resolution. The fitting procedure used to extract the B lifetimes from our sample of neutral B mesons and our sample of charged B mesons comes next (sections 6 and 7). The fit results on the individual lifetimes are given in section 8, and the systematic uncertainties are discussed in section 9. The results on the lifetime ratio and the corresponding systematic uncertainties are discussed in section 10.

A preliminary analysis of a subset of the dataset used for this analysis is documented in references [4, 5].

2 The decay length difference technique

At an asymmetric B Factory the $\Upsilon(4S)$ decay products are Lorentz boosted and fly long enough for their flight paths to be comparable to the experimental resolution. Since no charged stable particles emerge from the $\Upsilon(4S)$ decay point, the decay length of the individual B mesons is unknown and we determine the B lifetimes from the difference between the decay lengths of the two B mesons in an event.

The z axis of the *BABAR* coordinate system is defined to be parallel to the magnetic field in the solenoid [6]. Suppose the boost of the machine was parallel to the z axis and the B mesons were produced exactly at threshold in $\Upsilon(4S)$ decays. The B momenta in the $\Upsilon(4S)$ rest frame would be zero. Define $z_{\rm rec}$ and $z_{\rm opp}$ as the z coordinates of the decay points of the fully reconstructed and the opposite B, respectively. We call $\Delta z = z_{\rm rec} - z_{\rm opp}$ the signed decay length difference. Under the above assumptions, $|\Delta z|$ is distributed exponentially with an average of $\langle|\Delta z|\rangle = (\beta\gamma)_B c\tau_B = p(4{\rm S})/M(4{\rm S}) \cdot c\tau_B$. Complications arise from several effects. The axis of the PEP-II beams is tilted by 20 mrad with respect to the z axis [6], and the energies of the beams fluctuate, giving the $\Upsilon(4S)$ momentum a gaussian distribution with a standard deviation of 6 MeV/c [7]. Furthermore, the energy release in the $\Upsilon(4S) \to B\overline{B}$ decay makes the B mesons move in the $\Upsilon(4S)$ rest frame. The latter effect has the highest impact on the Δz distribution of our events, but all of these effects are small compared to the experimental resolution on Δz [7].

The topology of the events is sketched in figure 1. It is not drawn to scale. The opening angle between the trajectories of the B mesons is generally non-zero because of the energy release in $\Upsilon(4S) \to B\overline{B}$, and it is always smaller than 214 mrad [8]. The flight paths are of the order of 260 μm and the errors on $z_{\rm rec}$ and $z_{\rm opp}$ are usually of the order of 50 μm and 110 μm, respectively. Figure 2 shows the theoretical Δz distribution for two extreme cases: flight direction of the two Bs orthogonal to the z axis in the centre-of-mass frame, and both Bs flying along the z axis in the centre-of-mass frame.

For the present analysis we reconstruct Δz, i.e. the difference of the projections of the decay paths on the z axis, and the angle of the fully reconstructed B's flight direction with respect to the beam direction, measured in the centre-of-mass frame. The average boost $\vec{\beta}_{\Upsilon(4S)}$ of the centre-of-mass frame is measured on a run by run basis using 2-prong events [9]. We then use the "average τ_B approximation" [10] to estimate the difference Δt of the two proper decay times from these quantities, and extract the B lifetimes from fits to the experimental Δt distributions. Even in the absence of measurement errors, this Δt calculation is not exact. The common production point of the two B mesons needs to be known for an exact calculation of Δt [10]. This approximation leads to a bias on the measured lifetime that does not average out completely in the integration over all possible configurations. The residual bias is small, however (see section 9.7). This procedure, using only the projections of the B flight paths and of the boost of the centre-of-mass frame, automatically takes into account the systematic tilt of the beam axis with respect to the z axis [10].

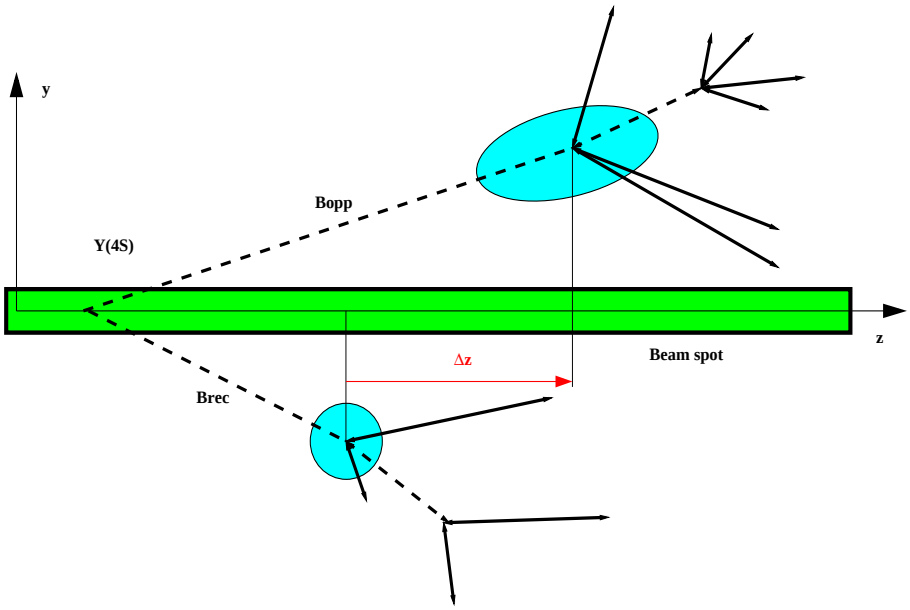

Figure 1: Event topology. The figure is not drawn to scale (see text).

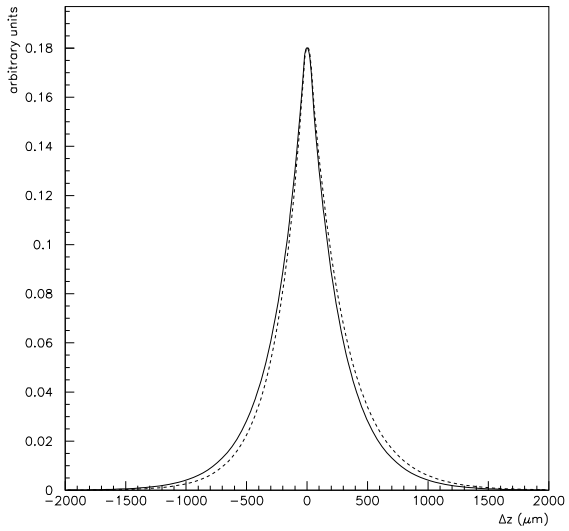

Figure 2: Theoretical Δz distribution for $\tau_B = 470$ μm and $(\beta\gamma)_{\Upsilon(4S)} = 0.556$. The solid curve is for a purely transverse $\Upsilon(4S)$ decay. The dashed line is for a decay with $(\beta\gamma)_{\rm rec} = 0.497$ and $(\beta\gamma)_{\rm tag} = 0.615$.

3 Detector and dataset

The *BABAR* detector is described elsewhere [11]. For this measurement, the most important subdetectors are the silicon vertex tracker (SVT) and the central drift chamber (DCH) which provide tracking and the electromagnetic calorimeter (EMC) from which photons and π^0s are reconstructed. The charged particle momentum resolution is approximately $(\delta p_T/p_T)^2 = (0.0015\, p_T)^2 + (0.005)^2$, where p_T is in GeV/c. The SVT, with a typical single-hit resolution of 10 μm provides vertex information in both the transverse plane and in z. The precision on charged particle momenta, neutral particle energies and spatial coordinates from the tracking and calorimetry lead to resolutions on invariant masses and other kinematical quantities which allow a clean separation of the complex decay trees we reconstruct (see section 4). Impact parameter resolutions in the transverse plane are $\simeq 50\,\mu$m at high momentum, and better than 100 μm for $p_T > 0.6$ GeV/c in the longitudinal (z) coordinate.

Particle identification facilitates the reconstruction of complex decay modes and of decays to J/ψ final states. Leptons and hadrons are identified using a combination of measurements from all the *BABAR* components, including the energy loss $\mathrm{d}E/\mathrm{d}x$ using a truncated mean of 40 samples (maximum) in the DCH and 5 samples in the SVT. Electrons and photons are identified in the barrel and the forward regions by the CsI electromagnetic calorimeter (EMC). Muons are identified in the instrumented flux return (IFR). In the central polar region, the Cerenkov ring imaging detector (DIRC) provides $> 3\sigma$ kaon identification for B decay products in the high momentum range where $\mathrm{d}E/\mathrm{d}x$ is no longer sensitive.

The data used in this analysis were collected with the *BABAR* detector at the PEP-II storage ring in the periods October - November, 1999 and February - October, 2000. The total integrated luminosity of the dataset is 20.7 fb^{-1} collected near the $\Upsilon(4S)$ resonance and 2.6 fb^{-1} collected 40 MeV below the $\Upsilon(4S)$ resonance [12, 13]. The corresponding number of produced $B\bar{B}$ pairs is estimated to be 23×10^6 [14].

We use the runs flagged as "good" by the Run Quality Manager [12]. Not all of these data were taken and reconstructed under the same conditions. Roughly half of the data included in this analysis were taken with the DCH operating at 1900 V, the other half with the DCH high voltage at 1960 V (see table 1). The data were processed with three different SVT local alignment sets (see table 2). In addition, several different software releases were used. For a more detailed break-down of the dataset, see [12].

	on peak	off peak
DCH HV at 1900 V	11.2 fb^{-1}	1.3 fb^{-1}
DCH HV at 1960 V	9.5 fb^{-1}	1.4 fb^{-1}
Total	20.7 fb^{-1}	2.6 fb^{-1}

Table 1: Break-down of the dataset into subsets taken with the DCH operating at the same high voltage.

	on peak	off peak
SVT LA set A	0.4 fb^{-1}	-
SVT LA set C	3.2 fb^{-1}	0.3 fb^{-1}
SVT LA set D	5.7 fb^{-1}	0.6 fb^{-1}
SVT LA set E	11.4 fb^{-1}	1.7 fb^{-1}
Total	20.7 fb^{-1}	2.6 fb^{-1}

Table 2: Break-down of the dataset into subsets processed with the same SVT local alignment set.

4 Reconstruction of hadronic B decays

This section outlines the first step of this analysis, the reconstruction of B candidates.

In section 4.1 we list the decay modes we reconstruct. The reconstruction procedure and the selection criteria we use are described in detail in other *BABAR* analysis documents [15, 16]. In section 4.2 we just give a brief summary that focuses on a few aspects that are most relevant to the lifetime measurements. The final sample of reconstructed B candidates is described in section 4.3.

4.1 Decay modes reconstructed

The modes we reconstruct are listed in table 3. Here, and throughout this document, we use the convention that a particular candidate state also implies that the charge conjugate state is included. In the same way, reference to a decay chain like

$$\overline{B}^0 \to D^{*+}\pi^-; D^{*+} \to D^0\pi^+; D^0 \to K^-\pi^+$$

also implies that the charge conjugate decay chain is included.

The modes we reconstruct are clean two body decays to states that include either a charmed meson or a charmonium meson. The mesons including a c quark are reconstructed in their cleaner decay modes. As B branching fractions tend to be small and the D or J/ψ branching fractions further reduce the yield for a given decay chain, we need to "add many drops in the bucket". We reconstruct 20 B^0 decay chains, including 2 that contain a J/ψ. In addition, we reconstruct 13 B^+ decay chains, including 6 that contain a J/ψ or a $\psi(2S)$.

4.2 Reconstruction techniques

The reconstruction procedure and the selection criteria we use are described in detail in [15, 16]. These selection criteria include a cut on the χ^2 probability of a topological vertex fit for the following intermediate states: a_1^+, K_S^0, D^0 and D^+. No cuts on the χ^2 probability of topological or kinematical fits of B candidates are applied.

If there are multiple candidates per event, only the one with the smallest ΔE is retained. This criterion is also used to choose among overlapping candidates in different decay modes, including the cases where one of the two B candidates is neutral and the other one is charged.

$\overline{B^0}$		
	$D^{*+}\pi^-$, $D^{*+} \to D^0\pi^+$	$D^0 \to K^-\pi^+$ $D^0 \to K^-\pi^+\pi^0$ $D^0 \to K^0_S\pi^+\pi^-$ $D^0 \to K^-\pi^+\pi^-\pi^+$
	$D^{*+}\rho^-$, $D^{*+} \to D^0\pi^+$ $\rho^- \to \pi^-\pi^0$	$D^0 \to K^-\pi^+$ $D^0 \to K^-\pi^+\pi^0$ $D^0 \to K^0_S\pi^+\pi^-$ $D^0 \to K^-\pi^+\pi^-\pi^+$
	$D^{*+}a_1^-$, $D^{*+} \to D^0\pi^+$ $a_1^- \to \rho^0(\to \pi^+\pi^-)\pi^-$	$D^0 \to K^-\pi^+$ $D^0 \to K^-\pi^+\pi^0$ $D^0 \to K^0_S\pi^+\pi^-$ $D^0 \to K^-\pi^+\pi^-\pi^+$
	$D^+\pi^-$	$D^+ \to K^-\pi^+\pi^+$ $D^+ \to K^0_S\pi^+$
	$D^+\rho^-$	$D^+ \to K^-\pi^+\pi^+$ $D^+ \to K^0_S\pi^+$
	$D^+a_1^-$	$D^+ \to K^-\pi^+\pi^+$ $D^+ \to K^0_S\pi^+$
	$J/\psi\,\overline{K^{*0}}$, $J/\psi \to \ell^+\ell^-$	$\overline{K^{*0}} \to K^-\pi^+$ $(\ell^+\ell^- = \{e^+e^-,\, \mu^+\mu^-\})$
B^-		
	$D^0\pi^-$	$D^0 \to K^-\pi^+$ $D^0 \to K^-\pi^+\pi^0$ $D^0 \to K^0_S\pi^+\pi^-$ $D^0 \to K^-\pi^+\pi^-\pi^+$
	$D^{*0}\pi^-$, $D^{*0} \to D^0\pi^0$	$D^0 \to K^-\pi^+$ $D^0 \to K^-\pi^+\pi^0$ $D^0 \to K^-\pi^+\pi^-\pi^+$
	$J/\psi\,K^-$, $J/\psi \to \ell^+\ell^-$ $\psi(2S)K^-$, $\psi(2S) \to J/\psi(\to \ell^+\ell^-)\pi^+\pi^-$ $\psi(2S) \to \ell^+\ell^-$	

Table 3: Reconstructed hadronic decay chains.

4.3 Sample composition

The substituted mass spectrum of our sample of B^0 candidates is shown in figure 3. A fit to the sum of the Argus background function [17] and a gaussian to model the signal is superimposed. From this fit, we estimate the number of signal candidates to be 6967 ± 95, with a purity of $\simeq 90\%$. All purities quoted in this section are calculated for the region within $\pm 2\sigma$ of the fitted B mass. The corresponding plot for the B^+ sample is shown in figure 4. The number of signal candidates is 7266 ± 94 with a purity of $\simeq 93\%$. The yields for each B decay mode are listed in table 4.

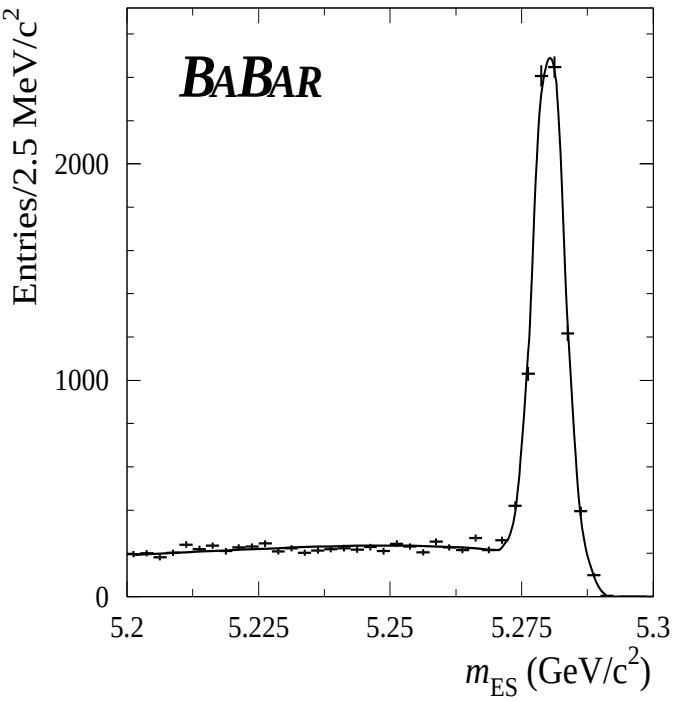

Figure 3: Substituted mass spectrum of the candidates in our B^0 sample.

The dominant contribution to the background in our samples comes from the decay modes to open charm. We run the same reconstruction and selection procedure for these modes on all available generic Monte Carlo [18]. The substituted mass spectra, including a break-down of the different contributions to the background are shown in figures 5 and 6. The background compositions in the substituted mass sideband and in the signal region are summarised in table 5.

Figures 5 and 6 also include a fit to the sum of the Argus background function and a gaussian. The difference between the histogram for background events and the fitted Argus function is shown in figures 7 and 8. We fit a function of the form constant plus gaussian to these histograms to estimate the fraction of "peaking background" in our samples. For this fit, we fix the width and the mean of the gaussian at the values from the fit shown in figures 5 and 6. The constant and the surface of the gaussian are free parameters. The values of the constant obtained from the fits to both samples are consistent with zero, and the fitted surfaces correspond to 71 ± 21 events for the neutral B sample and 87 ± 20 events for the

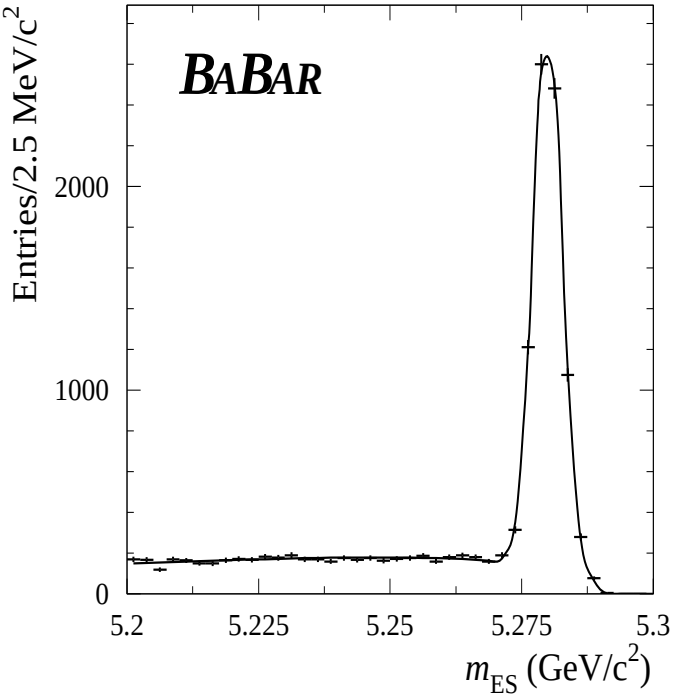

Figure 4: Substituted mass spectrum of the candidates in our B^+ sample.

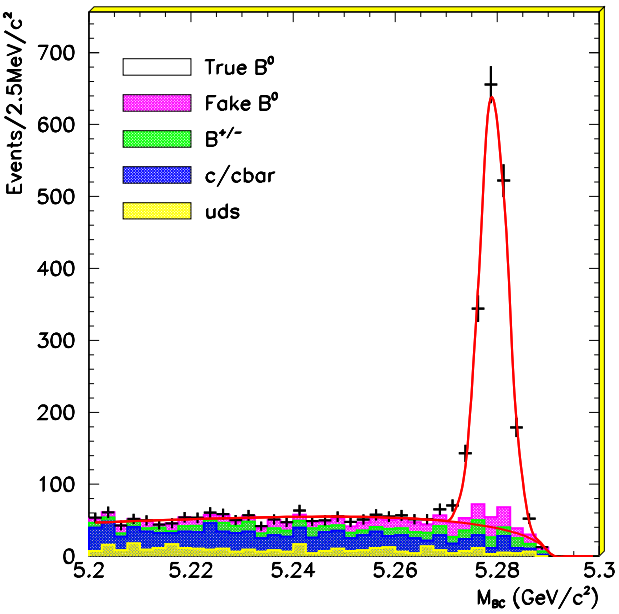

Figure 5: Substituted mass spectra of selected B^0 candidates on generic Monte Carlo. A fit to Argus+gaussian is superposed. The number of events in the gaussian is 1685 ± 49.

Table 4: B^0 and B^- signal yields and corresponding purities estimated from fits to the $m_{\rm SE}$ distributions.

Decay mode	Number of signal candidates	S/(S+B) [%]
$B^0 \to D^{*-}\ \pi^+$	1568 ± 42	95
$B^0 \to D^{*-}\ \rho^+$	898 ± 37	88
$B^0 \to D^{*-}\ a_1^+$	723 ± 32	86
$B^0 \to D^-\ \pi^+$	1768 ± 46	91
$B^0 \to D^-\ \rho^+$	900 ± 37	83
$B^0 \to D^-\ a_1^+$	526 ± 29	80
$B^0 \to J/\psi\ K^{*0}$	580 ± 25	98
$B^- \to D^0\ \pi^-$	4527 ± 75	91
$B^- \to D^{*0}\ \pi^-$	1180 ± 38	94
$B^- \to J/\psi\ K^-$	1355 ± 38	98
$B^- \to \psi(2S)\ K^-$	210 ± 15	98
Total B^0	6967 ± 95	90
Total B^-	7266 ± 94	93

		Same B species	Other B species	$c\overline{c}$	$uds/\overline{uds}$
B^0:	Sideband I ($5.2 < m_{\rm ES} < 5.225$)	15.7 ± 1.6 %	12.1 ± 1.4 %	49.0 ± 2.2 %	23.2 ± 1.9 %
	Sideband II ($5.235 < m_{\rm ES} < 5.26$)	20.6 ± 1.8 %	17.4 ± 1.7 %	43.2 ± 2.2 %	18.9 ± 1.8 %
	Signal ($m_{\rm ES} > 5.27$)	39.2 ± 2.6 %	25.0 ± 2.6 %	24.7 ± 2.2 %	11.2 ± 1.6 %
B^+:	Sideband I ($5.2 < m_{\rm ES} < 5.225$)	11.0 ± 1.6%	7.2 ± 1.3 %	53.1 ± 2.6 %	28.8 ± 2.3 %
	Sideband II ($5.235 < m_{\rm ES} < 5.26$)	12.6 ± 1.6 %	7.2 ± 1.2 %	51.4 ± 2.4 %	28.9 ± 2.2 %
	Signal ($m_{\rm ES} > 5.27$)	40.0 ± 2.6 %	20.0 ± 2.1 %	27.4 ± 2.4 %	12.6 ± 1.8 %

Table 5: Break-down of the background contributions to the hadronic sample (generic Monte Carlo).

charged B sample: 4 ± 1 % of our neutral B "signal" and 5 ± 1 % of our charged B "signal" are peaking background. Figures 9 and 10 show the two different $b\overline{b}$ contributions to the background in the B^0 and the B^+ sample, respectively. This information is also included in figures 5 and 6, but the peaking background is easier to see in figures 9 and 10. The latter figures indicate that both in the case of the B^0 sample and the B^+ sample, at least two thirds of the peaking background come from the "correct" B species. The mechanisms that lead to peaking background (soft π^+/π^0 exchange) are discussed in [15]. To a good approximation, the lifetime of the peaking background due to $B^0/\overline{B}^0$ events is that of the B^0 meson, and that of peaking background due to $B^\pm$ events is that of the B^+ meson [15].

5 Vertex reconstruction and Δt resolution function

The next step after the reconstruction of the B mesons and the event selection is the reconstruction of Δt, the observable we use as input to the lifetime fit. The event topology is

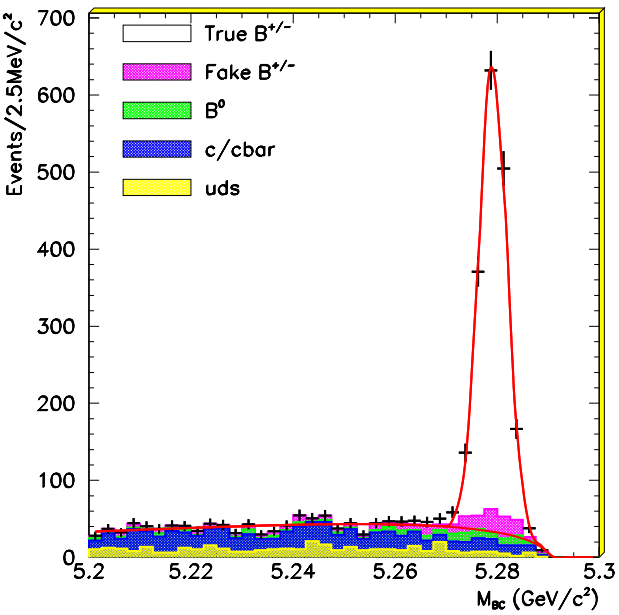

Figure 6: Substituted mass spectra of selected B^+ candidates on generic Monte Carlo. A fit to Argus+gaussian is superposed. The number of events in the gaussian is 1662 ± 49.

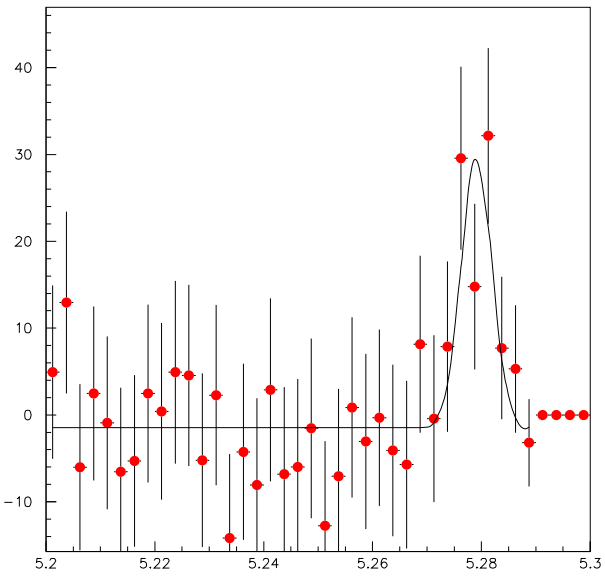

Figure 7: Difference of histogram for background and fitted Argus function shown in figure 5.

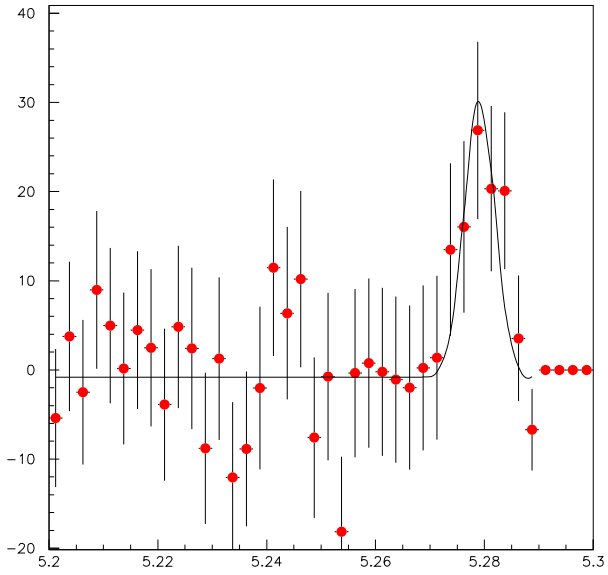

Figure 8: Difference of histogram for background and fitted Argus function shown in figure 6.

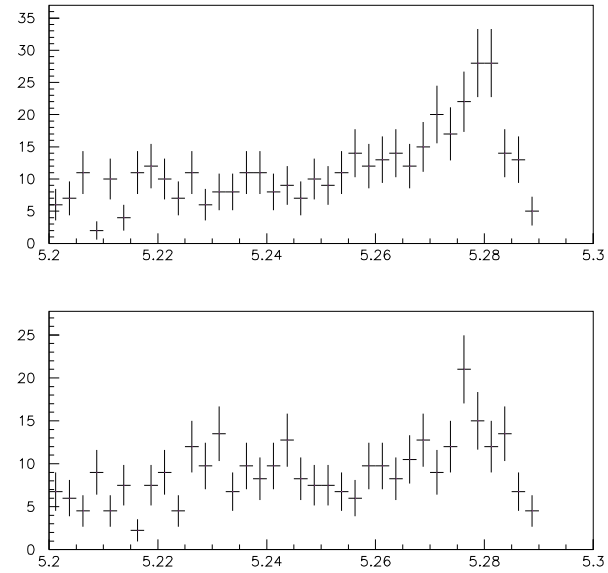

Figure 9: The background contributions from $B^0/\overline{B}^0$ events (top plot) and $B^{\pm}$ events (bottom plot) to the B^0 sample, which are also included in figure 5, shown individually.

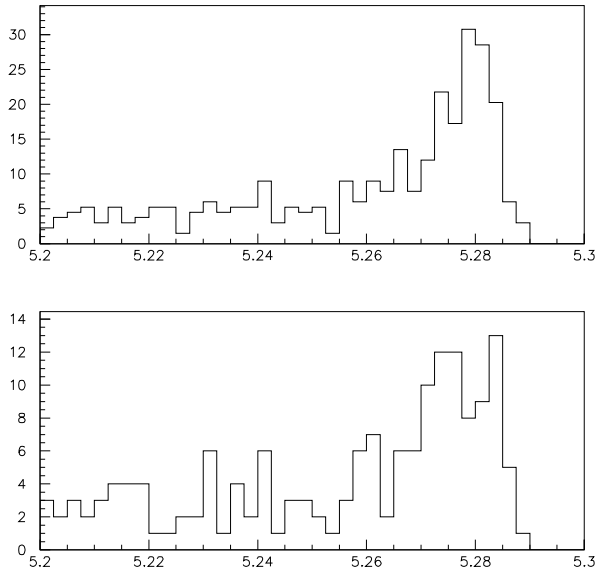

Figure 10: The background contributions from $B^{\pm}$ events (top plot) and $B^0/\overline{B}^0$ events (bottom plot) to the B^+ sample, which are also included in figure 6, shown individually.

sketched in figure 1 and the general strategy to measure the lifetime using Δt was discussed in section 2.

In measurements that use the decay length difference technique, it is more difficult to disentangle the effects of the lifetime and the detector resolution than in analyses where both the production and decay points of the particle in question are measured. In the latter analyses, the true proper decay times are distributed exponentially. In theory, there should be no events at negative decay times. The negative part of the measured decay time distribution contains valuable information on the detector resolution. The width of the negative part tells us about the resolution, the positive part contains the combined effect of resolution and lifetime. For the decay time difference Δt, theory predicts a distribution that is symmetric around $\Delta t = 0$. The width of the distribution resulting from the convolution of the theoretical distribution with the resolution function carries information about the combined effect of the lifetime and the detector resolution. The information necessary to separate the two effects is in the form of the distribution. A detailed understanding of the resolution function is crucial for lifetime measurements using the decay length difference technique. We need to learn as much as possible from data about the resolution function.

In sections 5.1 and 5.2 we discuss the reconstruction of the vertices of the two B mesons in an event. The Δt resolution function is discussed in section 5.3.

$\sigma(\Delta z) < 400\ \mu$m
$\lvert\Delta z\rvert < 3000\ \mu$m
$n_{\text{track}} \geq 2$

Table 6: Quality cuts applied after Δz reconstruction.

5.1 Vertex of the fully reconstructed B

We use the GeoKin algorithm [10] to reconstruct the vertex of the fully reconstructed B.

5.2 Opposite vertex

We use the VtxTagBtaSelFit algorithm with $n = 0$ [10] to reconstruct the opposite vertex. Table 6 lists the quality cuts we apply.

5.3 Δt resolution function

Figure 11 shows the distribution of the per-event error on Δt for data and Monte Carlo. Figure 12 shows the Δt pull obtained from signal Monte Carlo.

5.3.1 Shape

The resolution function is asymmetric due to the presence of secondary tracks from charm. For a more detailed discussion, see [4].

5.3.2 Parameterisation

Figure 12 includes the results of fits to the "GExp" resolution model (defined in section 6.1). The fitted parameter values are given in table 7. The results of fits of double gaussians to the same distribution are shown in figure 13 and summarised in table 8.

5.3.3 Outliers

For a small fraction of events, on the order of a few per mil in Monte Carlo, Δt is very poorly reconstructed, with residuals up to tens of picoseconds or up to 30 times the estimated uncertainty. Figure 14 shows the Δt residual distribution of such *outlier* events in neutral Supercocktail Monte Carlo. The "hole" in the middle of the distribution is a feature introduced by the cut on pull(Δt) used to identify these events. The solid line in figure 14 represents the result of a fit of a gaussian (also with a "hole" in the middle) to the distribution of Δt residuals. From this fit, the width of the distribution is estimated to be on the order of 7.2 ± 0.9 (stat) ps and the mean on the order of -0.2 ± 0.5 (stat) ps. The corresponding width and mean for the charged Supercocktail are 7.6 ± 1.1 (stat) ps and -1.2 ± 0.6 (stat) ps, respectively.

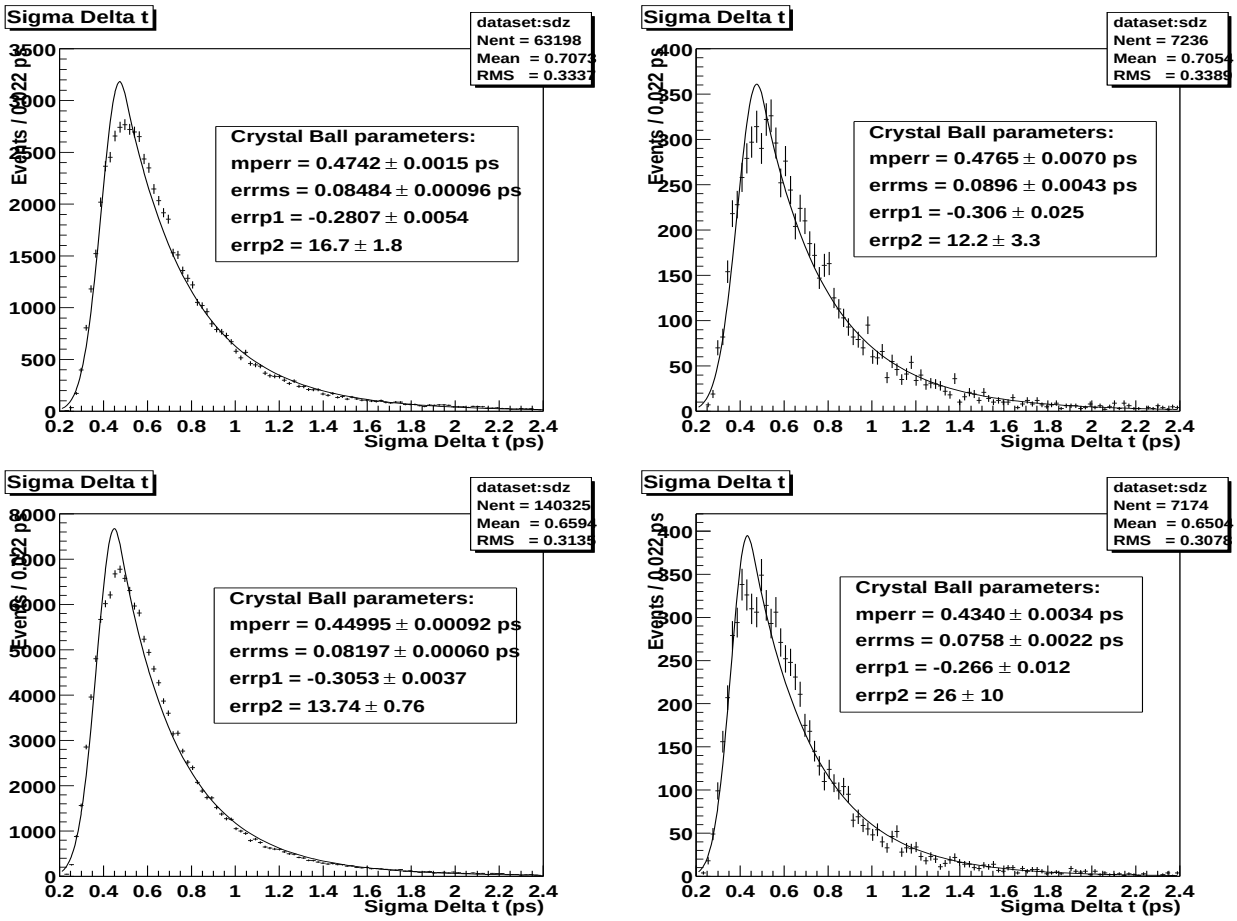

Figure 11: Per-event error on Δt for $B^0/\overline{B}^0$ events (top) and $B^{\pm}$ events. Left: Monte Carlo, right: data.

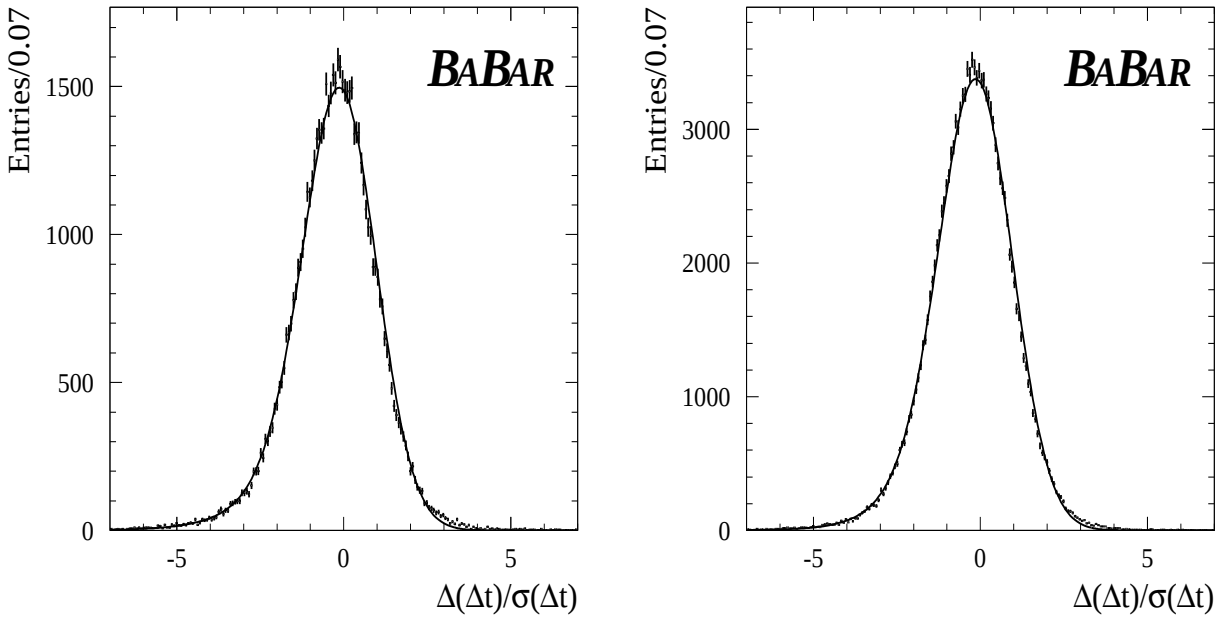

Figure 12: Δt pull for neutral (left) and charged (right) Supercocktail Monte Carlo. The solid line represents the result of a fit to the "GExp" parameterisation. The fitted parameter values are included in table 7.

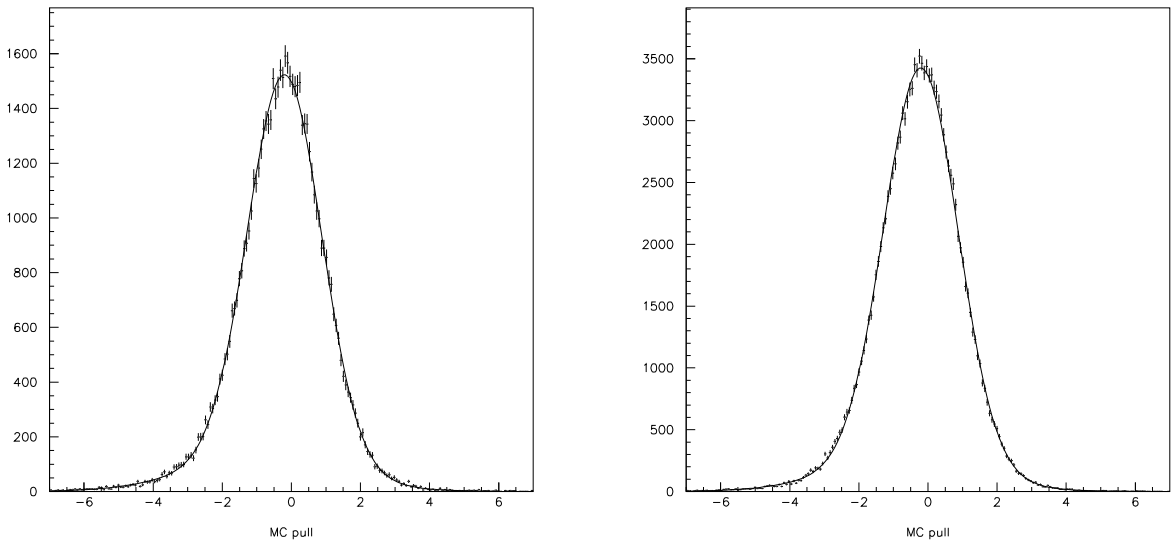

Figure 13: Δt pull for neutral (left) and charged (right) Supercocktail Monte Carlo. The solid line represents the result of a fit to the sum of two gaussians. The fitted parameter values are summarised in table 8.

B →	D* →	D →	s	$\tau_{\rm r}$	g	RMS
$\overline{B}^0$						
$D^{*+}\pi^-$	$D^0\pi^+$	$K^-\pi^+$	1.06 ± 0.03	0.589 ± 0.099	0.503 ± 0.090	1.30
$D^{*+}\pi^-$	$D^0\pi^+$	$K^-\pi^+\pi^0$	1.07 ± 0.03	1.22 ± 0.22	0.734 ± 0.050	1.41
$D^{*+}\pi^-$	$D^0\pi^+$	$K^-\pi^+\pi^-\pi^+$	1.03 ± 0.02	0.882 ± 0.098	0.600 ± 0.052	1.34
$D^{*+}\pi^-$	$D^+\pi^0$	$K^-\pi^+\pi^+$	1.03 ± 0.02	0.614 ± 0.074	0.484 ± 0.067	1.26
$D^{*+}\rho^-$	$D^0\pi^+$	$K^-\pi^+\pi^0$	1.03 ± 0.03	1.09 ± 0.24	0.657 ± 0.067	1.35
$D^{*+}\rho^-$	$D^0\pi^+$	$K^-\pi^+\pi^-\pi^+$	1.02 ± 0.04	0.524 ± 0.144	0.416 ± 0.166	1.31
$D^{*+}a_1^-$	$D^0\pi^+$	$K^-\pi^+\pi^-\pi^+$	1.04 ± 0.03	0.773 ± 0.184	0.591 ± 0.097	1.28
$D^+\pi^-$		$K^-\pi^+\pi^+$	1.03 ± 0.01	0.967 ± 0.059	0.693 ± 0.024	1.34
$D^+\pi^-$		$K^0_S\ \pi^+$	0.99 ± 0.04	0.774 ± 0.288	0.748 ± 0.099	1.26
$D^+\rho^-$		$K^0_S\ \pi^+$	1.06 ± 0.05	1.34 ± 0.61	0.734 ± 0.085	1.29
$D^+a_1^-$		$K^-\pi^+\pi^+$	0.96 ± 0.02	1.29 ± 0.16	0.741 ± 0.035	1.36
B^-						
$D^0\pi^-$		$K^-\pi^+$	1.01 ± 0.08	0.756 ± 0.029	0.620 ± 0.018	1.25
$D^0\pi^-$		$K^-\pi^+\pi^0$	1.05 ± 0.01	0.719 ± 0.048	0.653 ± 0.029	1.25
$D^0\pi^-$		$K^-\pi^+\pi^-\pi^+$	1.03 ± 0.01	0.800 ± 0.037	0.643 ± 0.020	1.25
$D^{*0}\pi^-$	$D^0\pi^0$	$K^-\pi^+$	1.04 ± 0.02	0.732 ± 0.076	0.659 ± 0.041	1.26
$D^{*0}\pi^-$	$D^0\pi^0$	$K^-\pi^+\pi^0$	1.04 ± 0.02	0.880 ± 0.106	0.712 ± 0.043	1.27
$D^{*0}\pi^-$	$D^0\gamma$	$K^-\pi^+$	1.01 ± 0.02	0.761 ± 0.070	0.662 ± 0.041	1.24
$D^{*0}\pi^-$	$D^0\gamma$	$K^-\pi^+\pi^0$	1.01 ± 0.03	0.515 ± 0.117	0.498 ± 0.119	1.25
	charmonium					
$\overline{B}^0$						
$J/\psi\ \bar{K}^{*0}$	e^+e^-	$\bar{K}^{*0} \to K^-\pi^+$	1.00 ± 0.03	0.979 ± 0.214	0.703 ± 0.070	1.42
B^-						
$J/\psi\ K^-$	e^+e^-		1.04 ± 0.01	0.810 ± 0.066	0.701 ± 0.031	1.29
$J/\psi\ K^-$	$\mu^+\mu^-$		1.01 ± 0.01	0.791 ± 0.047	0.592 ± 0.029	1.26
$\psi(2S)K^-$	$\pi^+\pi^-\ J/\psi$	$\ell^+\ell^-$	0.95 ± 0.03	0.646 ± 0.157	0.581 ± 0.107	1.26

Supercocktails:

	s	$\tau_{\rm r}$	g	Outlier fraction
Neutral Bs	1.063 ± 0.005	1.027 ± 0.021	0.709 ± 0.008	(0.45 ± 0.05) %
Charged Bs	1.057 ± 0.003	0.881 ± 0.015	0.685 ± 0.007	(0.21 ± 0.02) %

Table 7: Results of fits of the GExp resolution model to the Δt pulls obtained for various individual decay modes (not all of which are used in this analysis), as well as for the charged and neutral Supercocktails (all modes used in this analysis weighted according to the PDG2000 [1] branching fractions) [24]. (*The numbers for the supercocktails are for the latest vertexing, the table for the individual modes needs to be redone*)

Parameter	neutral Supercocktail	charged Supercocktail
fraction of events incentral gaussian	0.872 ± 0.006	0.893 ± 0.004
width_1	1.076 ± 0.006	1.080 ± 0.004
mean_1	-0.197 ± 0.006	-0.202 ± 0.004
width_2	2.298 ± 0.040	2.189 ± 0.026
mean_2	-0.913 ± 0.039	-0.845 ± 0.027

Table 8: Results of fits of the sum of two gaussians to the Δt pulls for the charged and neutral Supercocktails (see figure 13).

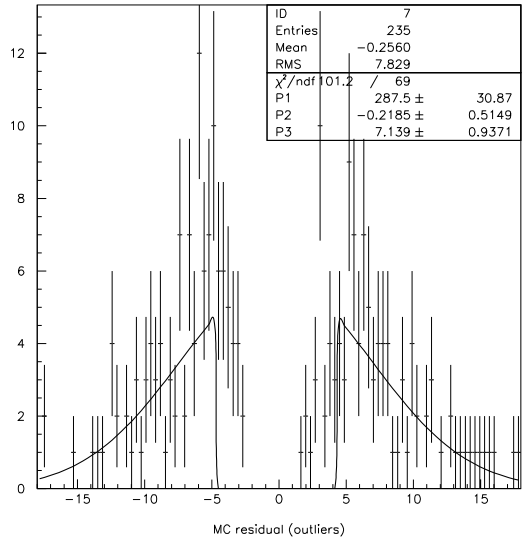

Figure 14: Δt residual for events in the neutral Supercocktail outside $-7.5 \leq \text{pull}(\Delta t) \leq 5.5$ (outliers).

6 Lifetime fitting procedure

The measurement technique has been outlined in section 2. We reconstruct Δt and extract the B meson lifetimes from the Δt distribution of the selected events using an unbinned maximum likelihood fit. The present section describes the unbinned maximum likelihood fit. We perform a simultaneous fit to the sample of reconstructed neutral B mesons and to the sample of reconstructed charged B mesons. Sections 6.1-6.3 describe how we construct the likelihood function for one B species. Section 6.4 summarises this likelihood function and describes how we combine the two likelihood functions for the two individual species and how we perform the combined fit.

We implement the combined maximum likelihood fit using the `RooFitTools` package [25], which uses Minuit [26] to perform the maximisation of the likelihood function numerically. The likelihood function involves several convolutions that are all done analytically. The formulae resulting from the corresponding integrations, as well as some mathematical pathologies encountered along the way and how to circumvent them, are also discussed in [25].

We use all selected events that contain a fully reconstructed B candidate with 5.20 GeV $< m_{\rm ES} <$ 5.29 GeV as input to the fit. There is no explicit distinction between sideband events and events in the signal region. We assign a signal probability $p_{{\rm sig},i}$ to each event i. It is based on the substituted mass of the fully reconstructed B candidate in the event. The Δt probability density function (PDF) for one event is a sum of two contributions. One to model the signal events in our data sample, and one for the background. Each of these two contributions contains a term that models outliers (see section 5.3.3). The signal contribution is discussed in section 6.1, and the background in section 6.2. The modelling of outliers is discussed in section 6.3.

6.1 Signal modelling

The theoretical Δt distribution consists of two exponential wings:

$$\phi(\Delta t;\tau_B) = \frac{1}{2\tau_B}\cdot\begin{cases}\exp\left(\frac{1}{\tau_B}\cdot\Delta t\right) & \Delta t \le 0\\ \exp\left(-\frac{1}{\tau_B}\cdot\Delta t\right) & \Delta t > 0\ .\end{cases}$$

To obtain the PDF $\Phi(\Delta t)$ for the reconstructed Δt in a given event number i, we convolute the theoretical distribution $\phi(\Delta t;\tau_B)$ with the resolution function $\mathcal{R}(\delta(\Delta t),\sigma_i)$, where $\delta(\Delta t)$ denotes the Δt residual and σ_i the error on Δt, estimated event by event.

$$\Phi(\Delta t) = \phi(\Delta t;\tau_B)\otimes\mathcal{R}(\delta(\Delta t),\sigma_i) = \int_{-\infty}^{\infty}\phi\left(\overline{\Delta t}\right)\cdot\mathcal{R}\left(\Delta t-\overline{\Delta t},\sigma_i\right)\ d\left(\overline{\Delta t}\right)$$

As discussed in section 5.3, the Δt residual is not normally distibuted. We assume a certain functional form for $\mathcal{R}(\delta(\Delta t),\sigma_i)$ that contains additional parameters. These parameters will be let free in the fit for τ_B to avoid extracting their values from Monte Carlo. In section 5.3 we saw that we need to introduce enough free parameters to give our function the flexibility to reproduce the effect of measurement errors. The parameters in the resolution function tend

to be strongly correlated to τ_B. Fitting simultaneously for correlated parameters increases the statistical error on all parameters. Quantitative examples of this effect can be found in section 7.

We study different parameterisations of the resolution function. One of them uses two gaussians ("G+G"):

$$\begin{aligned}\mathcal{R}(\delta(\Delta t),\sigma_i;f,s_1,b_1,s_2,b_2) &= f\cdot\frac{1}{\sqrt{2\pi}\cdot\sigma_i s_1}\cdot\exp\left(-\frac{(\delta(\Delta t)-b_1)^2}{2\sigma_i^2 s_1^2}\right)\\ &\quad +(1-f)\cdot\frac{1}{\sqrt{2\pi}\cdot\sigma_i s_2}\cdot\exp\left(-\frac{(\delta(\Delta t)-b_2)^2}{2\sigma_i^2 s_2^2}\right)\end{aligned}$$

It contains five parameters: the fraction of events in the first gaussian (f), the width (s_1) and mean (b_1) of the first gaussian and the width (s_2) and mean (b_2) of the second gaussian.

A different parameterisation uses one gaussian with variable width and zero bias plus the same gaussian convoluted with an exponential ("GExp"):

$$\begin{aligned}\mathcal{R}(\delta(\Delta t),\sigma_i;g,s,\tau_{\rm r}) &= g\cdot\frac{1}{\sqrt{2\pi}\cdot\sigma_i s}\cdot\exp\left(-\frac{(\delta(\Delta t))^2}{2\sigma_i^2 s^2}\right)\\ &+ (1-g)\cdot\frac{1}{2\cdot\sigma_i\tau_{\rm r}}\cdot\left[\exp\left(\frac{s^2}{2\tau_{\rm r}^2}+\frac{\delta(\Delta t)}{\sigma_i\tau_{\rm r}}\right)\cdot{\rm erfc}\left(\frac{s}{\sqrt{2}\tau_{\rm r}}+\frac{\delta(\Delta t)}{\sqrt{2}\cdot\sigma_i s}\right)\right]\ .\end{aligned}$$

It contains three parameters: the fraction g of events in the central gaussian, the width s of the gaussian and the "lifetime" $\tau_{\rm r}$ of the exponential.

6.2 Background modelling

We extract most of the information on the background properties from events in the substituted mass sideband. Figure 15 is a histogram of Δt for events with a $B^0/\overline{B}^0$ candidate in the substituted mass region between 5.20 GeV and 5.26 GeV. All modes are combined and the same cut on ΔE is applied as for the selection of signal events. The solid line represents the result of an unbinned maximum likelihood fit of the function

$$\begin{aligned}B(\Delta t,\sigma_i;\kappa,\Lambda,g_{\rm B},s_{\rm B},\tau_{\rm r,B}) = [\kappa\cdot\phi(\Delta t;\Lambda)+(1-\kappa)\ \cdot\delta_{\rm Dirac}(\Delta t)]\\ \otimes\mathcal{R}(\delta(\Delta t),\sigma_i;g_{\rm B},s_{\rm B},\tau_{\rm r,B})\end{aligned}$$

to the Δt distribution of these sideband events. This function is the sum of a symmetric decay time difference distribution with a "lifetime" Λ and a Dirac delta function, both convoluted with the same resolution function of the "GExp" type.

The background is essentially combinatorial with contributions from both $b\overline{b}$ and continuum events; in particular $c\overline{c}$ events which are an abundant source of real D and D^* mesons. The background events from continuum tend to have small or zero "lifetimes", while background events from $b\overline{b}$ can have "lifetimes" of the same order of magnitude as the B lifetimes. Because of the machine boost, the Δt distribution of the background events is not necessarily symmetric around $\Delta t = 0$. We let all five parameters free in the above fit.

The results of the above fit are summarised in figure 15. The errors on the fit parameters are large, but our goal is not the precise determination of some parameter describing some

background property. We only need a fitted function that reproduces the background Δt distribution.

The corresponding histogram of Δt for events that contain a $B^{\pm}$ candidate in the substituted mass sideband region is shown in figure 16. It shows the same features as the histogram for $B^0/\overline{B}^0$.

In our maximum likelihood fit for τ_B, we use the same parameterisation $B(\Delta t, \sigma_i; \kappa, \Lambda, g_{\rm B}, s_{\rm B}, \tau_{\rm r,B})$ as in the independent fits discussed above. All five parameters are free. In the fit for τ_B we do not explicitly distinguish between events in the signal region and sideband events. Instead, we assign a signal probability to each event depending on the substituted mass of the fully reconstructed B candidate it contains. The sideband events, however, still dominate the determination of the parameters that describe the background.

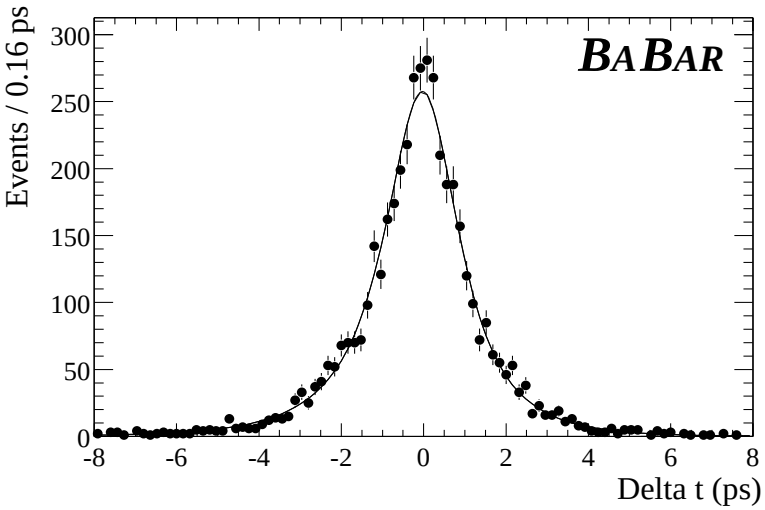

κ	=	0.326 ± 0.045
Λ	=	1.156 ± 0.096 ps
$g_{\rm B}$	=	0.881 ± 0.025
$s_{\rm B}$	=	1.355 ± 0.039
$\tau_{\rm r,B}$	=	1.69 ± 0.25
$f_{\rm out,B}$	=	0.61 ± 0.24 %

Figure 15: Δt distribution for events in the substituted mass sideband. All $B^0/\overline{B}^0$ modes combined. $\chi^2/\text{ndof} = 110.0/(100-6) = 1.17$ calculated from binned histogram and the result of the unbinned maximum likelihood fit. For the same distribution on logarithmic scale, see figure 17.

6.3 Outliers

Our Δz reconstruction quality cuts include the requirement that $|\Delta z| < 3000$ μm (see table 6). Neglecting the energy release in the $\Upsilon(4S)$ decay, this corresponds to $|\Delta t| < 17.9$ ps. Between $\Delta t = -17.9$ ps and $\Delta t = 17.9$ ps, we use a wide gaussian with a fixed width of $\sigma_{\rm out} = 10$ ps and fixed mean of $b_{\rm out} = 0$ ps to model the contribution of outliers to the total Δt distribution (see figure 14).

We model the Δt distribution of both background outlier events and signal outlier events with the type of gaussian described above. But we introduce two distinct parameters for the fraction of outliers among background events and the fraction of outliers among signal events: $f_{\rm out,B}$ and $f_{\rm out,S}$, respectively. These contributions to the PDF are properly normalised to take into account the cutoff at $|\Delta t| = 17.9$ ps.

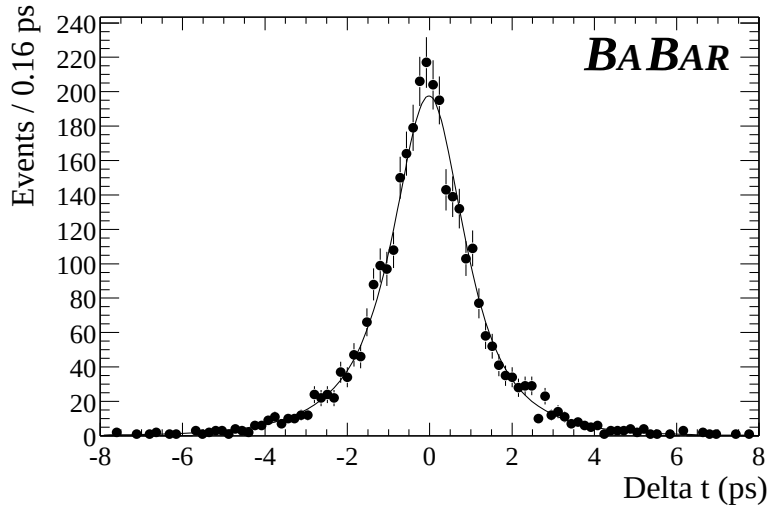

κ	=	0.295 ± 0.051
Λ	=	1.112 ± 0.123 ps
g_{B}	=	0.922 ± 0.032
s_{B}	=	1.399 ± 0.042
$\tau_{\mathrm{r,B}}$	=	1.52 ± 0.43
$f_{\mathrm{out,B}}$	=	0.67 ± 0.29 %

Figure 16: Δt distribution for events in the substituted mass sideband. All $B^{\pm}$ modes combined. $\chi^2/\mathrm{ndof} = 94.1/(100-6) = 1.00$ calculated from binned histogram and the result of the unbinned maximum likelihood fit. For the same distribution on logarithmic scale, see figure 17.

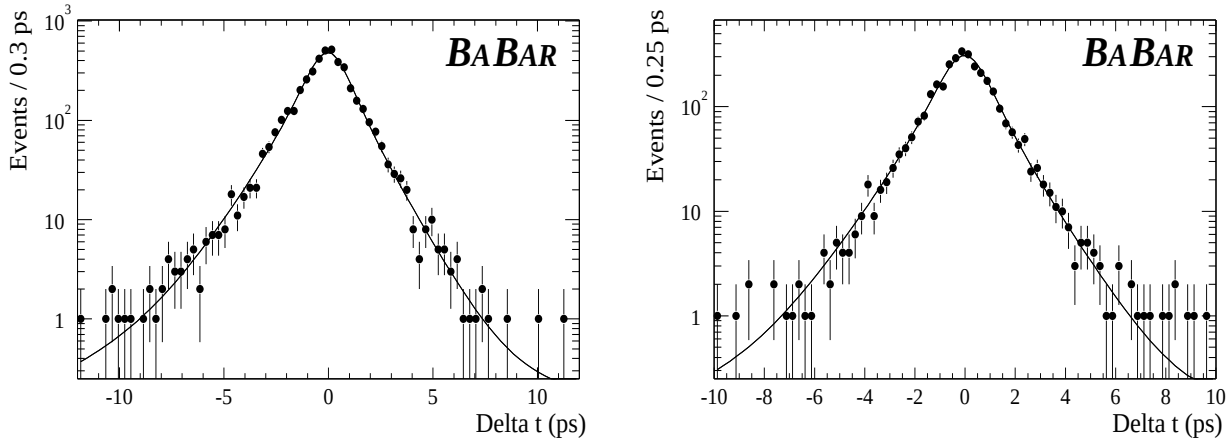

Figure 17: Same distributions as in figures 15 (left) and 16 (right), but plotted on logarithmic scale.

6.4 Likelihood function

We assign a signal probability $p_{\mathrm{sig},i}$ to each event i. It is based on the substituted mass of the fully reconstructed B candidate in the event and is derived from an independent fit of the Argus background function plus a gaussian to the substituted mass distribution of the fully reconstructed B candidates in our sample. One single fit to the substituted mass distribution of all B candidates of one species in our sample is performed, combining all modes. The purities for different modes that we reconstruct are different. This additional information could be exploited by taking into account the decay mode of the B candidate when calculating $p_{\mathrm{sig},i}$. In this case, fits to the substituted mass distributions for each mode need to be used. The background also needs to be modelled for each mode separately. This is a refinement that can be added easily once more statistics is available.

The negative log-likelihood function for one B species is

$$\begin{aligned}\mathcal{L} = -\sum_i \log\{ \quad & p_{\mathrm{sig},i} \cdot [(1-f_{\mathrm{out,S}}) \cdot \Phi\left((\Delta t)_i, \sigma_i; \{f, s_1, b_1, s_2, b_2\} \text{ or } \{g, s, \tau_{\mathrm{r}}\}\right) \\ & \qquad + f_{\mathrm{out,S}} \cdot O((\Delta t)_i; b_{\mathrm{out}}, \sigma_{\mathrm{out}})] \\ & (1-p_{\mathrm{sig},i}) \cdot [(1-f_{\mathrm{out,B}}) \cdot B((\Delta t)_i, \sigma_i; \kappa, \Lambda, g_{\mathrm{B}}, s_{\mathrm{B}}, \tau_{\mathrm{r,B}}) \\ & \qquad + f_{\mathrm{out,B}} \cdot O((\Delta t)_i; b_{\mathrm{out}}, \sigma_{\mathrm{out}})] \ \} \ ,\end{aligned}$$

where $O(\Delta t; b_{\mathrm{out}}, \sigma_{\mathrm{out}})$ denotes the outlier PDF discussed in section 6.3.

The measured variables for a given event i are $(\Delta t)_i$, the associated error σ_i and the signal probability $p_{\mathrm{sig},i}$. Both these input variables and the free parameters in the fit are summarised in table 9.

At the present level of statistical precision, the resolution functions for neutral and charged B s are compatible (section 5.3.1). We perform a combined fit to the Δt distributions of our two samples. The two Δt distributions are not combined. They are fitted simultaneously, but separately and with different sets of parameters to describe the background, the lifetime, etc. The only link between the two fits comes from the use of the same values for the parameters that describe the resolution function. Mathematically speaking, we minimise the sum of two terms of the form of $\mathcal{L}$, which have a subset of parameters in common.

7 Comparison of lifetime fits with different resolution models

Please see section 6 of BAD 130, version 2 [24].

8 Results of the fit to the data

In this section we present the fit results on the individual lifetimes, as well as some consistency checks.

Input variable		Description
$(\Delta t)_i$		proper decay time difference
σ_i		uncertainty on the proper decay time difference
$p_{\mathrm{sig},i}$		signal probability
Parameter		**Description**
τ_B		signal lifetime
Resolution function (signal):		
either	f	fraction of events in central gaussian
	s_1	width of central gaussian
	b_1	mean of central gaussian
	s_2	width of wide gaussian
	b_2	mean of wide gaussian
or	g	fraction of events in central gaussian
	s	width of gaussian
	τ_{r}	"lifetime" of the exponential that models the effect of the charm flight
Background:		
κ		fraction of background events which have a "lifetime"
Λ		"lifetime" of these events
Resolution function (background):		
g_{B}		fraction of events in central gaussian
s_{B}		width of gaussian
$\tau_{\mathrm{r,B}}$		"lifetime" of the exponential
Outliers:		
$f_{\mathrm{out,S}}$		fraction of outliers among signal events
$f_{\mathrm{out,B}}$		fraction of outliers among background events

Table 9: Description of input variables for each event and fit parameters used in the unbinned maximum likelihood lifetime fit. For the combined fit, we use two sets of signal lifetime, background and outlier parameters; but only one set of resolution parameters.

The unbinned maximum likelihood fits to the two $m_{\rm ES}$ spectra used to calculate the per-event signal probabilities are shown in figure 18. In these fits, both parameters of the Argus function, i.e. the endpoint and the shape parameter, are allowed to float. The number of neutral (charged) signal candidates is 6064 ± 88 (6336 ± 87).

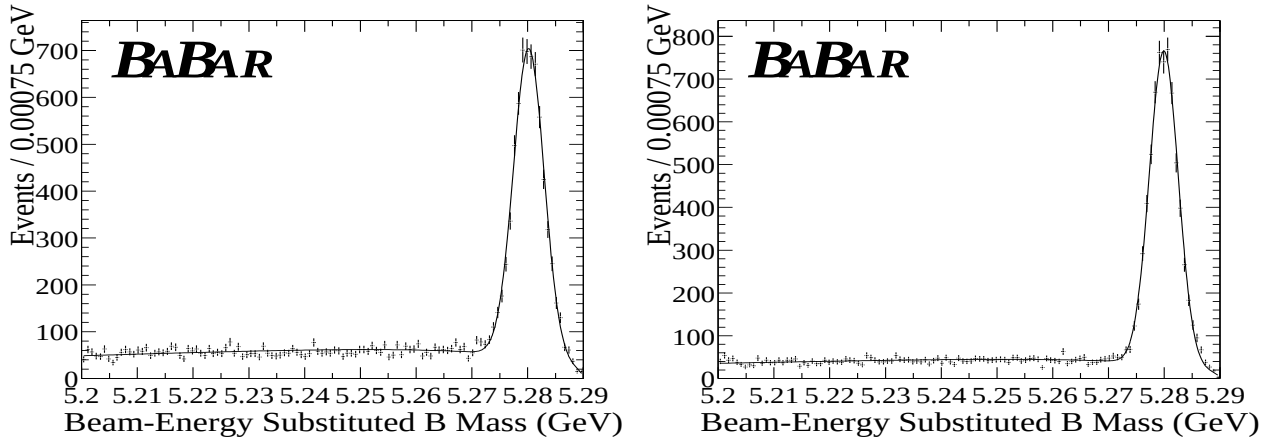

Figure 18: Substituted mass spectra for neutral (left) and charged (right) B candidates after Δt reconstruction and all quality cuts.

8.1 Result of the combined lifetime fit

Parameters:
1-2: centre and width of outlier gaussian (B^0)
3: B^0 lifetime
4-6: resolution function
7: $f_{\rm out,S}$ (in per mil), B^0 sample
8-9 and 18-20: B^0 candidate mass spectrum
10-17: background, B^0 sample
21-22: centre and width of outlier gaussian (B^+)
23: B^+ lifetime
24: $f_{\rm out,S}$ (in per mil), B^+ sample
25-26 and 35-37: B^+ candidate mass spectrum
27-34: background, B^+ sample

```
**********
**   17 **HESSE        6750
**********
COVARIANCE MATRIX CALCULATED SUCCESSFULLY
FCN=-3949.82 FROM HESSE     STATUS=OK             248 CALLS        1099 TOTAL
                    EDM=0.000328752    STRATEGY= 1      ERROR MATRIX ACCURATE
 EXT PARAMETER                                   INTERNAL      INTERNAL
 NO.   NAME      VALUE            ERROR          STEP SIZE       VALUE
  1  zentrum      0.00000e+00   constant
  2  breite       1.00000e+01   constant
  3  tauB         1.56041e+00   3.19692e-02   2.11329e-04   1.56041e+00
  4  sigma        1.20735e+00   6.97884e-02   4.38550e-04   1.20735e+00
  5  frac         6.91112e-01   7.35003e-02   5.50206e-04   3.92201e-01
  6  tau          1.03551e+00   2.44203e-01   5.37284e-04  -3.14834e-01
  7  outFrac      1.89556e+00   2.28400e+00   8.21070e-05  -1.48369e+00
  8  bmass        5.28019e+00     fixed
  9  bresn        2.73518e-03     fixed
```

```
 10  bOutBckg     0.00000e+00   constant
 11  sOutBckg     1.00000e+01   constant
 12  tauBckg      1.17068e+00   8.22751e-02   3.78276e-04   1.17068e+00
 13  sigmaBckg    1.34715e+00   3.71885e-02   1.98296e-04   1.34715e+00
 14  frBckg       8.94442e-01   2.21414e-02   1.16376e-04   8.94442e-01
 15  tauRBckg     1.74243e+00   2.63650e-01   1.37448e-03   1.74243e+00
 16  fLifeBckg    3.67457e-01   4.24344e-02   1.60185e-04   3.67457e-01
 17  fOutBckg     7.23832e+00   2.22448e+00   2.01324e-04  -1.40043e+00
 18  endpt        5.29078e+00     fixed
 19  c           -3.25892e+01     fixed
 20  f            4.81471e-01     fixed
 21  zentrumCh    0.00000e+00   constant
 22  breiteCh     1.00000e+01   constant
 23  tauBCh       1.67557e+00   3.17230e-02   2.12006e-04   1.67557e+00
 24  outFracCh    1.97793e+00   2.55096e+00   8.74602e-05  -1.48182e+00
 25  bmassCh      5.27992e+00     fixed
 26  bresnCh      2.57999e-03     fixed
 27  bOutBckgCh   0.00000e+00   constant
 28  sOutBckgCh   1.00000e+01   constant
 29  tauBckgCh    1.18151e+00   1.13096e-01   4.74244e-04   1.18151e+00
 30  sigmaBckgCh   1.38137e+00   3.88612e-02   2.18828e-04   1.38137e+00
 31  frBckgCh     9.14742e-01   3.19093e-02   1.57851e-04   9.14742e-01
 32  tauRBckgCh   1.41548e+00   3.75954e-01   1.82204e-03   1.41548e+00
 33  fLifeBckgCh   3.14255e-01   4.48627e-02   3.40528e-05   3.14255e-01
 34  fOutBckgCh   5.59549e+00   2.54636e+00   2.44585e-04  -1.42105e+00
 35  endptCh      5.29039e+00     fixed
 36  cCh         -3.29734e+01     fixed
 37  fCh          5.72333e-01     fixed
                               ERR DEF= 0.5
EXTERNAL ERROR MATRIX.    NDIM=  37    NPAR= 19    ERR DEF=0.5
 [covariance matrix omitted]

PARAMETER  CORRELATION COEFFICIENTS
      NO.  GLOBAL      3      4      5      6      7     12     13     14     15     16     17     23     24     29     30     31
       3  0.64802   1.000 -0.406 -0.179 -0.209 -0.376 -0.052  0.025  0.003  0.009 -0.003  0.020  0.270 -0.070 -0.005  0.019  0.008
       4  0.68988  -0.406  1.000 -0.216 -0.312  0.125 -0.001 -0.069 -0.002  0.009  0.017 -0.005 -0.325  0.103  0.003 -0.045 -0.004
       5  0.91794  -0.179 -0.216  1.000  0.911 -0.054  0.010  0.005 -0.059 -0.056 -0.008  0.008 -0.191  0.019  0.007  0.002 -0.045
       6  0.93301  -0.209 -0.312  0.911  1.000 -0.061  0.014  0.013 -0.038 -0.056 -0.008  0.009 -0.231  0.030  0.008  0.009 -0.030
       7  0.43389  -0.376  0.125 -0.054 -0.061  1.000  0.049 -0.000  0.003  0.005 -0.012 -0.128 -0.035  0.012  0.000 -0.005  0.001
      12  0.84793  -0.052 -0.001  0.010  0.014  0.049  1.000  0.318 -0.102 -0.237 -0.732 -0.333 -0.006  0.001  0.000 -0.000 -0.000
      13  0.78906   0.025 -0.069  0.005  0.013 -0.000  0.318  1.000  0.223  0.144 -0.679 -0.105  0.025 -0.007 -0.000  0.003  0.001
      14  0.79567   0.003 -0.002 -0.059 -0.038  0.003 -0.102  0.223  1.000  0.721  0.077 -0.088  0.008 -0.000 -0.000  0.001  0.004
      15  0.79965   0.009  0.009 -0.056 -0.056  0.005 -0.237  0.144  0.721  1.000  0.042 -0.155  0.015 -0.002 -0.000 -0.000  0.002
      16  0.90056  -0.003  0.017 -0.008 -0.008 -0.012 -0.732 -0.679  0.077  0.042  1.000  0.187 -0.005  0.002  0.000 -0.001  0.000
      17  0.46790   0.020 -0.005  0.008  0.009 -0.128 -0.333 -0.105 -0.088 -0.155  0.187  1.000 -0.001  0.000  0.000  0.000 -0.000
      23  0.63804   0.270 -0.325 -0.191 -0.231 -0.035 -0.006  0.025  0.008  0.015 -0.005 -0.001  1.000 -0.460 -0.040  0.010  0.007
      24  0.48075  -0.070  0.103  0.019  0.030  0.012  0.001 -0.007 -0.000 -0.002  0.002  0.000 -0.460  1.000  0.044  0.006  0.000
      29  0.87572  -0.005  0.003  0.007  0.008  0.000  0.000 -0.000 -0.000 -0.000  0.000  0.000 -0.040  0.044  1.000  0.338 -0.150
      30  0.76103   0.019 -0.045  0.002  0.009 -0.005 -0.000  0.003  0.001 -0.000 -0.001  0.000  0.010  0.006  0.338  1.000  0.226
      31  0.82174   0.008 -0.004 -0.045 -0.030  0.001 -0.000  0.001  0.004  0.002  0.000 -0.000  0.007  0.000 -0.150  0.226  1.000
      32  0.82994   0.011 -0.000 -0.035 -0.032  0.001 -0.000  0.000  0.002  0.002  0.000 -0.000  0.012 -0.002 -0.263  0.121  0.763
                    1.000  0.036 -0.013
      33  0.89930  -0.001  0.004 -0.005 -0.005  0.001 -0.000 -0.000  0.000  0.000  0.000 -0.000  0.004 -0.017 -0.758 -0.651  0.068
                    0.036  1.000  0.311
      34  0.56481  -0.000  0.000  0.000  0.000  0.000 -0.000 -0.000 -0.000 -0.000  0.000 -0.000  0.018 -0.077 -0.506 -0.154 -0.016
                   -0.013  0.311  1.000

**********
**   17 **MINOS        6750
**********
FCN=-3949.82 FROM MINOS     STATUS=SUCCESSFUL   8033 CALLS        8884 TOTAL
                    EDM=0.000328014    STRATEGY= 1      ERROR MATRIX ACCURATE
 EXT PARAMETER                  PARABOLIC          MINOS ERRORS
 NO.   NAME      VALUE            ERROR       NEGATIVE      POSITIVE
  1  zentrum      0.00000e+00   constant
  2  breite       1.00000e+01   constant
  3  tauB         1.56041e+00   3.19706e-02  -3.19807e-02   3.19924e-02
  4  sigma        1.20735e+00   6.97100e-02  -7.02189e-02   6.97340e-02
  5  frac         6.91112e-01   7.33590e-02  -9.45499e-02   6.28773e-02
  6  tau          1.03551e+00   2.43677e-01  -2.49307e-01   2.50141e-01
  7  outFrac      1.89556e+00   2.28588e+00   at limit      2.54410e+00
  8  bmass        5.28019e+00     fixed
  9  bresn        2.73518e-03     fixed
 10  bOutBckg     0.00000e+00   constant
 11  sOutBckg     1.00000e+01   constant
 12  tauBckg      1.17068e+00   8.24205e-02  -7.81033e-02   8.70327e-02
 13  sigmaBckg    1.34715e+00   3.71370e-02  -3.70415e-02   3.73773e-02
 14  frBckg       8.94442e-01   2.21446e-02  -2.33755e-02   2.10508e-02
 15  tauRBckg     1.74243e+00   2.63350e-01  -2.50643e-01   2.83076e-01
 16  fLifeBckg    3.67457e-01   4.24729e-02  -4.15267e-02   4.32411e-02
 17  fOutBckg     7.23832e+00   2.22387e+00  -2.05545e+00   2.39269e+00
 18  endpt        5.29078e+00     fixed
 19  c           -3.25892e+01     fixed
 20  f            4.81471e-01     fixed
 21  zentrumCh    0.00000e+00   constant
 22  breiteCh     1.00000e+01   constant
 23  tauBCh       1.67557e+00   3.17438e-02  -3.16967e-02   3.17861e-02
 24  outFracCh    1.97793e+00   2.55411e+00   at limit      2.79340e+00
 25  bmassCh      5.27992e+00     fixed
 26  bresnCh      2.57999e-03     fixed
 27  bOutBckgCh   0.00000e+00   constant
 28  sOutBckgCh   1.00000e+01   constant
 29  tauBckgCh    1.18151e+00   1.13286e-01  -1.07476e-01   1.19342e-01
```

```
 30  sigmaBckgCh   1.38137e+00   3.88205e-02  -3.88777e-02   3.88995e-02
 31  frBckgCh      9.14742e-01   3.19273e-02  -3.68870e-02   2.84180e-02
 32  tauRBckgCh    1.41548e+00   3.75600e-01  -3.59571e-01   4.11494e-01
 33  fLifeBckgCh   3.14255e-01   4.49296e-02  -4.27877e-02   4.70255e-02
 34  fOutBckgCh    5.59549e+00   2.54483e+00  -2.29693e+00   2.78721e+00
 35  endptCh       5.29039e+00      fixed
 36  cCh          -3.29734e+01      fixed
 37  fCh           5.72333e-01      fixed
                              ERR DEF= 0.5
```

Summary:

$\tau(B^0) = 1.560 \pm 0.032$ ps
$\tau(B^+) = 1.676 \pm 0.032$ ps

Resolution function:
$g = 0.69 \pm 0.07$
$\tau_{\rm r} = 1.04 \pm 0.24$
$s = 1.21 \pm 0.07$ (scale factor)

Outlier fraction:
B^0: $f_{\rm out,S} = 0.19 \pm 0.23$ %
B^+: $f_{\rm out,S} = 0.20 \pm 0.26$ %

Figures 19 and 20 show the Δt distributions for neutral and charged B candidates in the signal region. For the fit above, we do not make an explicit distinction between signal and sideband regions (see section 6). The plots in figures 19 and 20 include candidates in the region $\pm 2\sigma$ around the fitted B mass, as in section 4. Figure 21 shows the same distributions on a logarithmic scale.

The resolution function obtained from the fit above is in reasonable agreement with the Monte Carlo (see table 7). The scale factor obtained for Monte Carlo is about 1.06, the scale factor obtained for data is 2σ higher than that value. The standard Monte Carlo is produced with perfect detector alignment. Monte Carlo studies of the effect of various misalignments on the Δz reconstruction are documented in [24]. Studies of Δz control samples [27] find the errors on Δz in data to be $\simeq 15$ % worse than in Monte Carlo.

8.2 Consistency checks

Split the samples of B candidates into different subsets according to

- **B species (i.e. fit neutral and charged Bs separately)**
  The results of the combined fit and two separate fits to the sample of neutral Bs and to the sample of charged Bs are compared in table 10.

- **DCH voltage**
  We split the dataset into two subsamples with a given DCH high voltage (see table 1). We then use the combined lifetime fit to extract the two B lifetimes from each subsample. Two fits are performed to each subsample. In the first fit, all resolution parameters are free, and in the second fit the three parameters of the signal resolution function

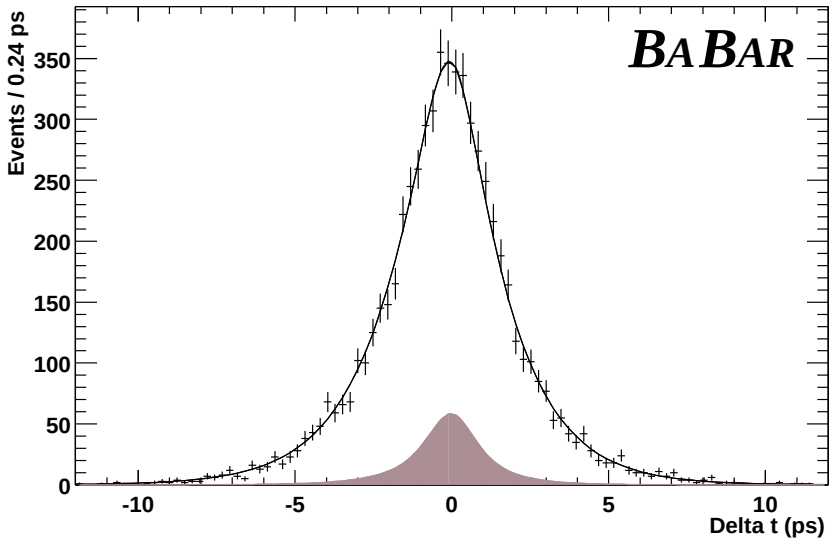

Figure 19: Δt distribution for $B^0/\overline{B}^0$ candidates in the signal region. The result of the lifetime fit is superimposed.

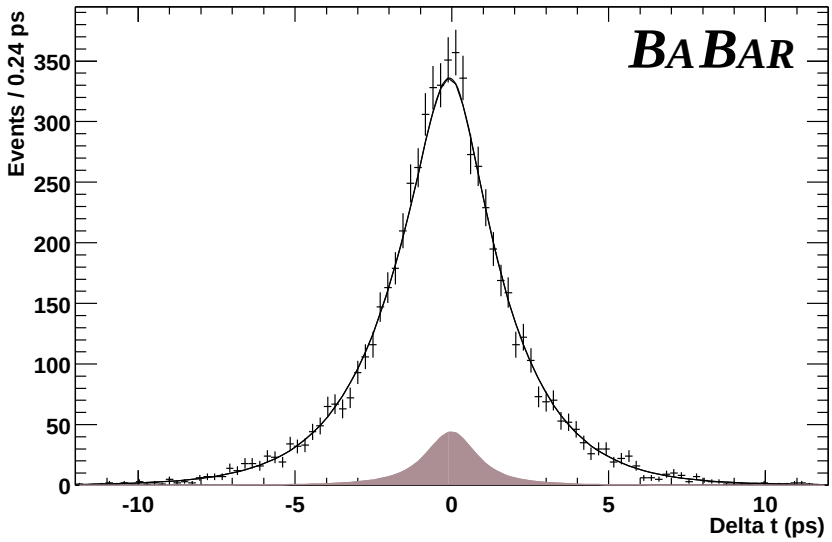

Figure 20: Δt distribution for $B^{\pm}$ candidates in the signal region. The result of the lifetime fit is superimposed.

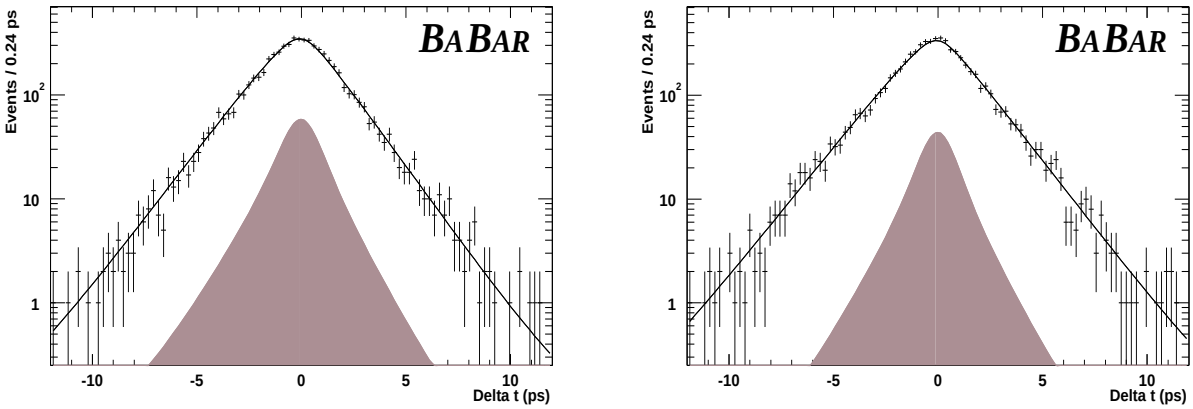

Figure 21: Same distributions as in figures 19 (left) and 20 (right), but plotted on logarithmic scale.

are fixed to the values obtained from the combined fit on the full sample. The results are listed in table 12.

- **Alignment set**
  Same game with different alignment sets: table 13.

- $B_{\rm rec}$ **decay mode**
  Table 11 shows the results of lifetime fits to subsamples that contain B candidates in a given subset of decay modes. Two fits are performed to each subsample. In the first fit, all resolution parameters are free, and in the second fit the three parameters of the signal resolution function are fixed to the values obtained from the full combined fit.

	combined fit	fit to $B^0/\overline{B}^0$ sample	fit to $B^\pm$ sample
$\tau(B^0)$	1.560 ± 0.032 ps	1.538 ± 0.036 ps	-
$\tau(B^+)$	1.676 ± 0.032 ps	-	1.698 ± 0.036 ps
g	0.69 ± 0.07	0.68 ± 0.15	0.69 ± 0.08
$\tau_{\rm r}$	1.04 ± 0.24	0.89 ± 0.40	1.14 ± 0.29
s	1.21 ± 0.07	1.34 ± 0.10	1.05 ± 0.11

Table 10: Summary of the results of the combined fit and individual fits to the sample of neutral Bs and to the sample of charged Bs. None of the corrections discussed in section 9 has been applied. In particular, the correction discussed in section 9.3 has not been applied to the results of the combined fit.

9 Systematic uncertainties

The decay length difference technique is different from various other methods used in other experimental environments, e.g. at SLD, LEP and CDF. For example, the measurement is

Sample	free resolution function	resolution function fixed to result of full combined fit
$D^{*+}X^-$	1.491 ± 0.050 ps	1.553 ps
D^+X^-	1.538 ± 0.060 ps	1.573 ps
$J/\Psi K^{*0}$	1.600 ± 0.103 ps	1.551 ps
All $B^0/\overline{B^0}$	1.538 ± 0.036 ps	1.560 ps
$D^{*0}\pi^+$	1.784 ± 0.089 ps	1.715 ps
$D^0\pi^+$	1.678 ± 0.046 ps	1.678 ps
ΨK^+	1.678 ± 0.063 ps	1.635 ps
All $B^\pm$	1.698 ± 0.036 ps	1.675 ps

Table 11: Results of lifetime fits to subsamples that contain B candidates in a given subset of decay modes.

DCH high voltage	free resolution function	resolution function fixed to result of fit to full sample
1900 V	$\tau(B^0) = 1.561 \pm 0.045$ ps	$\tau(B^0) = 1.581$ ps
	$\tau(B^+) = 1.631 \pm 0.045$ ps	$\tau(B^+) = 1.647$ ps
1960 V	$\tau(B^0) = 1.550 \pm 0.045$ ps	$\tau(B^0) = 1.537$ ps
	$\tau(B^+) = 1.695 \pm 0.040$ ps	$\tau(B^+) = 1.686$ ps

Table 12: Results of combined lifetime fits to subsamples with given DCH high voltage.

SVT LA set	free resolution function	resolution function fixed to result of fit to full sample
C	$\tau(B^0) = 1.427 \pm 0.113$ ps	$\tau(B^0) = 1.541$ ps
	$\tau(B^+) = 1.496 \pm 0.091$ ps	$\tau(B^+) = 1.589$ ps
D	$\tau(B^0) = 1.618 \pm 0.066$ ps	$\tau(B^0) = 1.605$ ps
	$\tau(B^+) = 1.738 \pm 0.067$ ps	$\tau(B^+) = 1.724$ ps
E	$\tau(B^0) = 1.552 \pm 0.041$ ps	$\tau(B^0) = 1.539$ ps
	$\tau(B^+) = 1.684 \pm 0.036$ ps	$\tau(B^+) = 1.673$ ps

Table 13: Results of combined lifetime fits to subsamples with given SVT local alignment set.

made in z rather than in the transverse plane, the production point of the B mesons is unknown and there is no contamination from b baryons. Consequently, some of the systematic uncertainties are also different.

In this section, we discuss the systematic uncertainties in our lifetime measurements using hadronic decay modes. These systematics can be grouped in three categories: uncertainties due to (1) the selection criteria used to obtain the data samples, (2) the Δt reconstruction and (3) the fitting procedure.

The first category is discussed in section 9.1, the second one in sections 9.2-9.7 and the third one on sections 9.8-9.10. The systematic uncertainties are summarised and combined in section 9.11.

9.1 Sample selection

In general, selection criteria can bias the decay time distribution of candidates in the final sample. For example, quality cuts can produce such an effect if candidates with long decay times reach regions in the detector where the spatial resolution is significantly worse than at the interaction region. We do not expect this particular effect to be large for Bs in *BABAR*.

We apply the full event reconstruction and candidate selection procedure on signal Monte Carlo. The effect of an inconsistency in one of the decay files [28, 29] has been corrected for using the recipe described in [29]. We check the generated Δt spectrum of events that pass all our selection cuts for distortions. Table 14 summarises the results of unbinned maximum likelihood fits of the theoretical Δt distribution to the generated Δt spectra of the event samples that pass our selection cuts. We use the result of the unbinned likelihood fit and the binned histogram to perform a χ^2 test.

These checks do not show any evidence of a significant distortion of the Δt spectrum. We use our full fitting procedure to extract the lifetimes from the reconstructed Δt distributions. The fitted lifetimes are consistent with the generated ones. We assign the statistical error from the combined fit as systematic uncertainty on our measurements on data ("MC statistics" in table 21).

9.2 Parameterisation of the resolution function

In measurements that use the decay length difference technique, the lifetime to be measured is strongly correlated to the resolution function. In this measurement, the largest systematic error comes from the fact that our knowledge of the Δt resolution in data is limited. We "transform a part of this systematic uncertainty into a contribution to the statistical error" by letting all parameters in the resolution function free during the lifetime fit. This uncertainty is already included in our statistical error. For illustration purposes, we repeat the combined lifetime fit fixing the parameters in the resolution function at the values obtained in the fit discussed section 8. The error on $\tau(B^0)$ ($\tau(B^+)$) is reduced from 0.032 ps (0.032 ps) to 0.027 ps (0.028 ps). The "difference in quadrature" is 0.018 ps (0.016 ps) or 1.1 % (0.9 %) of the PDG lifetime.

Additional uncertainties arise from the possibility that the parameterisation of the resolution function, despite its free parameters, is not "flexible" enough to reproduce all features

Lifetimes:

		using generated Δt		using reconstructed Δt	
	generated lifetime	fitted lifetime	χ^2/ndof	measured lifetime (separate fits)	measured lifetime (combined fit)
B^0	1.548 ps	1.5476 ± 0.0062 ps	208.2/199	1.5592 ± 0.0103 ps	1.5562 ± 0.0087 ps
B^+	1.653 ps	1.6521 ± 0.0044 ps	197.6/199	1.6627 ± 0.0071 ps	1.6647 ± 0.0065 ps

Fitted resolution functions:

	fit to B^0 sample	fit to B^+ sample	combined fit
g	0.723 ± 0.027	0.723 ± 0.028	0.724 ± 0.019
τ_r	1.01 ± 0.10	0.91 ± 0.09	0.95 ± 0.07
s	1.016 ± 0.026	1.030 ± 0.020	1.025 ± 0.016

Table 14: Checks of B decay time difference spectra after reconstruction/selection procedure.

of the "real" resolution function. To estimate the impact of such effects on the lifetime measurements, we generate 4000 toy MC samples with roughly the size of our data sample, using a more flexible resolution model, namely the G+G parameterisation. We use the values extracted from a fit to Supercocktail MC (see section 5.3.1) for generation. We then use the GExp model to fit for the lifetimes. The $B^0/\overline{B}^0$ ($B^\pm$) lifetime is overestimated by 0.0075 ± 0.0005 ps (0.0039 ± 0.0005 ps). We correct our measurements for this bias and assign the size of the correction as systematic uncertainty.

9.3 Identical resolution function

We use a combined fit to the Δt distributions of charged and neutral Bs to extract their lifetimes (see section 6). In this fit, we make the approximation of equal Δt resolution functions for all $B_{\rm rec}$ modes, regardless of the B species.

To estimate the size of a possible bias introduced by averaging the resolution functions for different $B_{\rm rec}$ modes for the same B species, we generate toy Monte Carlo samples for one species, where half of the sample is generated with a given set of values for the resolution function parameters, and the other half with a different set of given values for the resolution parameters. We then use a single resolution function to extract the lifetime. The values of the resolution parameters used for generation are those for the neutral B Supercocktail and the mode $B^0 \to D^-\pi^+$, $D^- \to K^0_S\pi^-$ taken from table 7. From 4000 toy Monte Carlo samples of 7000 events each, we estimate the bias on the lifetime to be 0.0006 ± 0.0006 ps.

To estimate the effect of the approximation of equal resolution functions for charged and neutral Bs, we generate 4000 toy Monte Carlo samples of 7000 charged plus 7000 neutral Bs each, with different resolution functions for charged and neutral Bs. The values for generation are those for the two Supercocktails from table 7. We then use our combined fitting procedure to extract the two lifetimes using a common resolution function for charged and neutral Bs. The generated lifetimes are taken from [1]. The fitted $\tau(B^0)$ is biased by 0.0040 ± 0.0006 ps towards higher values, and the fitted $\tau(B^+)$ is biased by 0.0052 ± 0.0006 ps towards lower values. We correct our measurements on data for these biases and assign the

size of the correction as systematic uncertainty.

9.4 Beam spot

VtxTagBtaSelFit, the algorithm we use to reconstruct Δt, makes use of our knowledge of the beam spot position and size to obtain a constraint on the opposite vertex [10]. A potential bias in the determination of the beam spot parameters [30] can change the Δt resolution function. The values of various parameters in the resolution function are determined from data in the lifetime fit (see section 6) and most changes to the resolution function are "absorbed" by the fit.

We use the full set of B^0 signal Monte Carlo to obtain a limit on any residual effects on the fitted lifetimes. We reconstruct the same set of events several times using different sets of beam spot parameters. Table 15 contains the changes of the fitted lifetimes we observe for different distortions of the beam spot: displacements of the beam spot in y ("offset") and random gaussian per-event smearings of the beam spot position in y ("error") to model a larger beam spot size. A shift of 50 μm in y is large compared to the observed movements of the beam spot over several consecutive runs [24]. Blowing up the beam spot to 20 μm or even 50 μm in y is a large variation: if the beam spot were that large, PEP-II could not deliver the luminosities it does [30]. The movements of the beam spot within one run have been studied in [31] for a typical run, and found to be less than 10 μm in y. We assign 0.0020 ps as systematic error on the lifetimes.

Change of beam spot parameters used for Δt reconstrunction	shift of fitted lifetime τ_B(distorted beam spot) $-$ τ_B(generated beam spot)
error 10 μm	-0.0008 ps
error 20 μm	-0.0020 ps
error 50 μm	-0.0052 ps
offset 10 μm	-0.0009 ps
offset 20 μm	$+0.0006$ ps
offset 50 μm	$+0.0010$ ps

Table 15: Effect of various distortions of the beam spot on the fitted lifetime for $\simeq 65k$ reconstructed events.

9.5 Δt outliers

The likelihood function for the lifetime fit contains a wide gaussian that models outliers (see section 6.3). The fractions of outliers in the B^0 and the B^+ sample are free parameters, whereas the width and mean of the gaussian are fixed at the values obtained from Monte Carlo. To estimate the impact of a possible difference in the Δt structure of outliers in data and Monte Carlo, we generate data-sized Toy Monte Carlo samples with different values for the width and the mean of the gaussian, and use the nominal lifetime fit to extract the B lifetime. Table 16 shows the bias of the fitted lifetime for different sets of values used at generation time. For each configuration, 2000 Toy Monte Carlo samples were generated, with a B lifetime of 1.548 ps.

Gaussians with a width of 15 ps or more are mostly flat in the region of interest ($|\Delta t| <$ 17.9 ps, see section 6.3). Outliers with a very narrow Δt distribution do not bias the lifetime significantly as most of them will not be in the region that contains most information on the B lifetime. Table 16 contains three columns for different values of the outlier fraction used at generation time. The 0.5 % fraction used for the last column is two thirds higher than the fraction seen in Monte Carlo and more than one sigma higher than the fractions extracted from the lifetime fit to the data.

We assign 0.0114 ps as systematic uncertainty on the B lifetimes.

		Frac = 0.2 %	Frac = 0.35 %	Frac = 0.5 %
Mean = 0 ps	Width = 15 ps	−0.0042 ps	−0.0061 ps	−0.0091 ps
	Width = 12 ps	−0.0012 ps	−0.0037 ps	−0.0031 ps
	Width = 8 ps	+0.0020 ps	+0.0059 ps	+0.0070 ps
	Width = 6 ps	+0.0030 ps	+0.0077 ps	+0.0114 ps
	Width = 4 ps	−0.0004 ps	+0.0031 ps	+0.0051 ps
Mean = 3 ps	Width = 10 ps	−0.0004 ps	−0.0003 ps	−0.0005 ps
Mean = -3 ps	Width = 10 ps	−0.0007 ps	−0.0018 ps	−0.0024 ps

Table 16: Shift of the fitted lifetime (τ_B(fitted) − τ_B(generated)) for different outlier Δt distributions used at generation time.

9.6 Detector geometry and alignment

Imperfections in the detector alignment can influence the Δz reconstruction and change the Δt resolution function. We determine the parameters in the parameterisation of the Δt resolution function from the data (see sections 6.1 and 9.2), and most alignment effects are automatically taken into account by this procedure. We study the effect of various misalignments in full Monte Carlo and set a limit on any residual effects on the reconstructed B lifetimes that cannot be reproduced by our parameterisation of the resolution function.

The technical aspects of this kind of study are discussed in [24]. Estimates of the size of various systematic features known to exist in the SVT local alignment sets that have been used to reconstruct the data (e.g. "telescope effect", shift of the outer layers with respect to the inner layers, etc.), as well as limits on other effects are discussed in [32, 33]. In addition, we study the effect of uncorrelated random displacements of all individual SVT wafers that model uncertainties due to statistical limitations of the local alignment procedure, and global misalignments of the SVT as a whole with respect to the DCH. Limits on the global misalignments are derived from the temporal evolution of the relevant alignment parameters [34]. A summary of all misalignments studied here can be found in table 17.

We reconstruct the same set of signal Monte Carlo events with perfect detector alignment and with the misalignments described above introduced into a conditions database proxy. We then use our fitting procedure to extract the B lifetime. Table 18 lists the shifts of the fitted lifetime with respect to the lifetime measured with perfect alignment. Only the events that are common to the two samples are taken into account. To reduce the number of events needed for this study, we determine the three resolution parameters (see section 6.1) from

a fit to the Δt residuals obtained using Monte Carlo truth information, and then fix them in the lifetime fits. The number of events in the final samples used for these fits is between 3.91k and 4.25k in all cases. We assign the sum in quadrature of the absolute value of the shifts listed in table 18 as systematic uncertainty.

Various alignment and calibration procedures use the data to estimate the size of relative displacements of different detector components. These procedures do not determine or adjust the global length scale of the experiment. A possible imperfection in the z scale of the detector directly biases the B lifetime measurements. One way to determine the z scale is to use the detector to measure the length in z of something with known dimensions. Such a measurement of the length of the Beryllium beam pipe [35] using protons from material interactions therein and in the Tantalum foil wrapped around it, is described in [36]. For alignment sets C, D and E, the scale factor $f = \frac{\text{length seen by detector}}{\text{length from independent measurement}}$ is consistent with one at the one to two per mil level. This z scale determination uses predominantly tracks that pass the extremities (in z) of the SVT. We do not expect the z scale for the inner regions of the SVT to be orders of magnitude worse than for the outer regions, and assign 0.5 % as uncertainty on the z scale in these alignment sets. We also use a small amount of data processed with alignment set A (see section 3). No length scale measurement is available for alignment set A, and we use the same upper limit (1 %) on z scale uncertainties in this alignment set as [4]. We assign $\frac{0.4\,\text{fb}^{-1}}{19.5\,\text{fb}^{-1}} \cdot 1.00\,\% + \frac{19.1\,\text{fb}^{-1}}{19.5\,\text{fb}^{-1}} \cdot 0.50\,\% = 0.51\,\%$ (see table 2) as systematic uncertainty on the B lifetimes.

9.7 Approximate Δt calculation and uncertainty on the average boost

As discussed in section 2, we use the "average τ_B approximation" [10] to convert our measurements of Δz and the polar angle of the fully reconstructed B in the centre-of-mass system to Δt. The $\Upsilon(4S)$ boost needs to be known to boost the fully reconstructed B to the centre-of-mass frame, and as direct input to the Δt calculation. Even in the absence of measurement errors, Δt can only be calculated using approximations. We use a generator-level study of 980k B^+/B^- events to estimate the size of possible biases introduced by this approximate calculation. The Monte Carlo generator [37] simulates the effects of the beam energy spread, the tilt of the average $\Upsilon(4S)$ boost with respect to the z axis, and the energy release in the $\Upsilon(4S)$ decay. The generated B^+ lifetime is 1.653 ps. Figure 22 shows the distribution of per-event differences between the generated Δt and the Δt calculated using the "average τ_B approximation" and the generated Δz, B momentum and the average generated $\Upsilon(4S)$ boost. The lifetime extracted from an unbinned maximum likelihood fit to the approximate Δt is 1.6544 ± 0.0017 ps. The lifetime extracted from the true Δt of the same events is 1.6518 ± 0.0017 ps. The smearing due to the "average τ_B approximation" broadens the Δt distribution. From the RMS in figure 22, we estimate this to introduce a bias on the fitted lifetime of the order of 0.2 %, unless the smearing is taken into account. In fits to reconstructed Δt distributions, this smearing broadens the resolution function and can at least partially be absorbed therein. The Δt pulls discussed in section 5 already contain this effect.

OPR measures $\vec{\beta}_{\Upsilon(4S)}$ from two-prong events. The accuracy on the boost direction is

`boostZ`:	"Telescope effect": R dependent shift of all SVT layers along z axis. The shift is larger for layers that are further away from the beam axis.
`boostZ_setD`:	The telescope effect is particularly large in SVT LA set D.
`outerShiftY005`:	Shifts of the outer two layers w.r.t. the inner layers (50 μm along y).
`ExpandZ001`:	$z \Rightarrow (1+\epsilon)z$, $\epsilon = 0.001$
`ExpandZ-001`:	$z \Rightarrow (1+\epsilon)z$, $\epsilon = -0.001$
`ExpandR0005`:	$x \Rightarrow (1+\epsilon)x$, $\epsilon = 0.0005$ $y \Rightarrow (1+\epsilon)y$ (increase SVT radius by 76 μm)
`TwistZ000002`:	$x = R\cos\phi \Rightarrow x = R\cos(\phi + \epsilon z)$, $\epsilon = 0.000002$ $y = R\sin\phi \Rightarrow y = R\sin(\phi + \epsilon z)$
`Ellips0014`:	$x = R\cos\phi \Rightarrow x = R\cos[(1+\epsilon\cos(2\phi))\phi]$, $\epsilon = 0.0014$ $y = R\sin\phi \Rightarrow y = R\sin[(1+\epsilon\cos(2\phi))\phi]$ (Note that only the position of the centre of individual SVT layers and the rotations of the wafers w.r.t. their nominal orientation are changed according to the transformations described above. The wafers themselves are not deformed.)
`LA101025`:	Random uncorrelated displacements of all individual SVT wafers. The translations in u (parallel to beam axis) and v (in the wafer plane, orthogonal to u) are normally distributed with $\sigma = 10$ μm. The translations in w are normally distributed with $\sigma = 25$ μm.
`globY10mu`:	Global shift (10 μm) of the SVT with respect to the DCH along the y axis.
`globZ40mu`:	Global shift (40 μm) of the SVT with respect to the DCH along the z axis.
`globRY002murad`:	Global rotation (2 μrad) of the SVT with respect to the DCH around the y axis.
`globRZ002murad`:	Global rotation (2 μrad) of the SVT with respect to the DCH around the z axis.

Table 17: A brief description of the "misalignment sets" used for this study.

Misalignment	Shift of reconstructed B lifetime
`boostZ`	-0.0016 ps
`boostZ_setD`	-0.0050 ps
`outerShiftY005`	-0.0004 ps
`ExpandZ001`	-0.0036 ps
`ExpandZ-001`	-0.0021 ps
`ExpandR0005`	-0.0003 ps
`TwistZ000002`	$+0.0017$ ps
`Ellips0014`	-0.0019 ps
`LA101025`	$+0.0010$ ps
`globY10mu`	$+0.0029$ ps
`globZ40mu`	-0.0012 ps
`globRY002murad`	$+0.0008$ ps
`globRZ002murad`	$+0.0016$ ps
Total in quadrature	0.0077 ps

Table 18: Shift of the reconstructed B lifetime [τ_B(reconstructed from Monte Carlo that includes misalignment) $-$ τ_B(reconstructed from Monte Carlo simulation of perfectly aligned detector)] for different misalignments. Exactly the same physics events have been used for the two Monte Carlo simulations. The sets `boostZ` and `boostZ_setD` describe the same effect, but with different amplitudes. The size of the corresponding bias is different for different SVT LA sets used to reconstruct the data (see table 2). The bias in all of the SVT LA sets is described by one of the two sets in this table. For the calculation of the sum, we simply take `boostZ_setD` which results in the larger shift of the lifetime. Idem for `ExpandZ001` and `ExpandZ-001`.

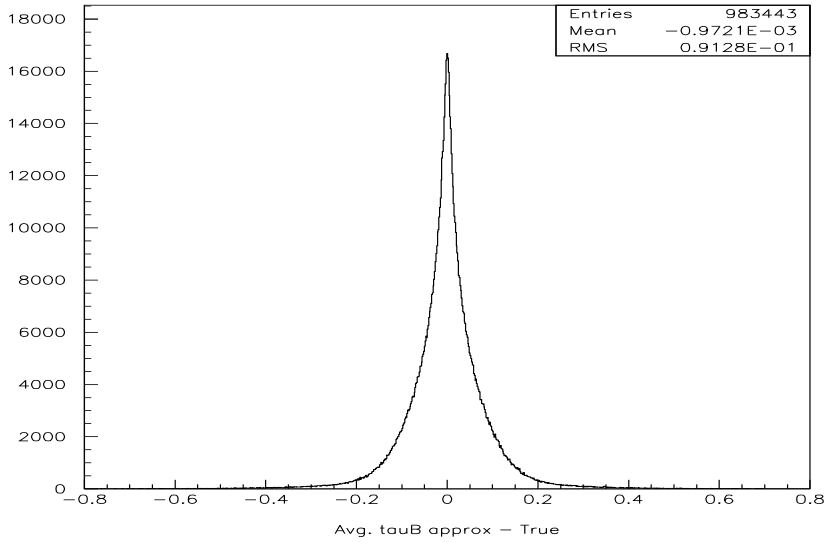

Figure 22: From generator-level study: per-event difference between true Δt and the Δt obtained using the "average τ_B approximation" in the absence of measurement errors.

of the order of 1 mrad, and the accuracy on $|\vec{\beta}_{\Upsilon(4S)}|$ is better than 0.3 % [38]. We repeat our generator-level study, varying $|\vec{\beta}_{\Upsilon(4S)}|$ by +0.3 % (−0.3 %) for the approximate Δt calculation. The lifetime extracted from the unbinned maximum likelihood fit changes to 1.6484±0.0017 ps (1.6607±0.0017 ps). This corresponds to a change of 0.0060 ps (0.0063 ps), or 0.38 % with respect to the value obtained with the true average boost. We assign 0.38 % as systematic uncertainty due to the approximate Δt calculation and the boost determination.

9.8 Signal probability

For the lifetime fit, we assign a signal probability to each event. It is based on the reconstructed substituted mass of the fully reconstructed B candidate contained in the event, and on an independent fit of Argus+gaussian to the $m_{\rm ES}$ spectrum of all B candidates of the same charge in the sample (see section 6). To propagate the errors from this independent fit to the lifetime fit, we repeat the lifetime fit varying the value of the (fixed) parameters that describe the $m_{\rm ES}$ spectra within one sigma from the independent fits to these spectra.

The change in the central value of the lifetime of one species introduced by the variation of any parameter of the $m_{\rm ES}$ distribution of the other B species is always smaller than 0.0003 ps. Varying the fraction of signal events in the B^0 (B^+) sample changes the corresponding lifetime by 0.0015 ps (0.0016 ps); varying the value of the Argus shape parameter changes the lifetime by 0.0016 ps (0.0019 ps). The variation of any other parameter changes the lifetime by less than 0.0004 ps (0.0007 ps).

We reconstruct B^0s in modes that contain a ρ resonance, and B^+s in modes that contain soft π^0s (see section 4). To estimate the impact of a possible tail of the signal $m_{\rm ES}$ distribution, we repeat the lifetime fit using a different function to model the $m_{\rm ES}$ spectra. Instead of

Argus+gaussian, we use Argus+Johnson $S_{\rm U}$ distribution [39]. For a certain choice of parameters, the latter distribution tends towards a gaussian, but it can also model a landau-like tail. The central value of the B^0 (B^+) lifetime changes by 0.0013 ps (0.0014 ps).

We assign the sum in quadrature of these three contributions as systematic uncertainty due to the uncertainties on the signal probability.

9.9 Background modelling

In section 4, we distinguish two types of backgrounds in our sample of fully reconstructed Bs: combinatorial background and peaking background. In this section we estimate the systematic uncertainties on the B lifetimes due to the presence of these backgrounds.

The combinatorial background is taken into account in the lifetime fit. A signal probability is assigned to each event, and the Δt distribution for background events is extracted from events in the $m_{\rm ES}$ sideband. The different sources of backgrounds in the $m_{\rm ES}$ sideband and in the $m_{\rm ES}$ signal region are listed in table 5. In this table, no distinction between peaking and combinatorial background is made. Table 19 shows the background composition in a slightly different way: the two sideband regions from table 5 have been combined and we no longer distinguish between $uds/\overline{uds}$ and $c\overline{c}$ or $B^0/\overline{B}^0$ and $B^\pm$. Furthermore, the estimate of the fraction of peaking background described in section 4 has been used to subtract the contribution from peaking background, assuming that all peaking background is due to $b\overline{b}$ events. Table 19 shows that the relative contributions from continuum and $b\overline{b}$ events to the combinatorial background are different for events in the sideband and in the signal region: combinatorial background in the signal region is enriched in $b\overline{b}$ events. If the Δt distributions for combinatorial background from continuum and $b\overline{b}$ events are not identical, then this leads to a systematic error on the measured B lifetimes.

		$b\overline{b}$	$udsc/\overline{udsc}$ (continuum)
B^0:	Sideband ($5.20 < m_{\rm ES} < 5.26$ GeV)	33.6 ± 1.7 %	66.4 ± 2.3 %
	Signal ($m_{\rm ES} > 5.27$ GeV)	53.3 ± 9.0 %	46.7 ± 4.0 %
B^+:	Sideband ($5.20 < m_{\rm ES} < 5.26$ GeV)	19.0 ± 1.4 %	81.0 ± 2.9 %
	Signal ($m_{\rm ES} > 5.27$ GeV)	46.6 ± 9.4 %	53.4 ± 4.5 %

Table 19: Break-down of the background contributions to the hadronic sample (generic Monte Carlo). The peaking component (see section 4) in the signal region has been subtracted.

The Δt distributions for background from continuum events with $5.20 < m_{\rm ES} < 5.30$ GeV and $b\overline{b}$ events with $5.20 < m_{\rm ES} < 5.26$ GeV (generic Monte Carlo) are shown in figure 23. The solid line in the plots for continuum background represents a fit to the sum of a Dirac delta function convoluted with a two gaussian resolution function that is used to scale the per-event error, and a gaussian centered at zero with a fixed width of 10 ps to model outliers. The five parameters of the resolution function, as well as the outlier fraction are free parameters in the fit. The solid line in the plots for $b\overline{b}$ background represents a fit to the sum of a function

of the form $\phi(\Delta t;\tau)$ (see section 6.1), convoluted with a one gaussian resolution function that scales the per-event error, and a 10 ps gaussian to model outliers. The parameter τ, the scale factor of the resolution function and the outlier fraction are free parameters in the fit. The parameter values from these fits are summarised in table 20.

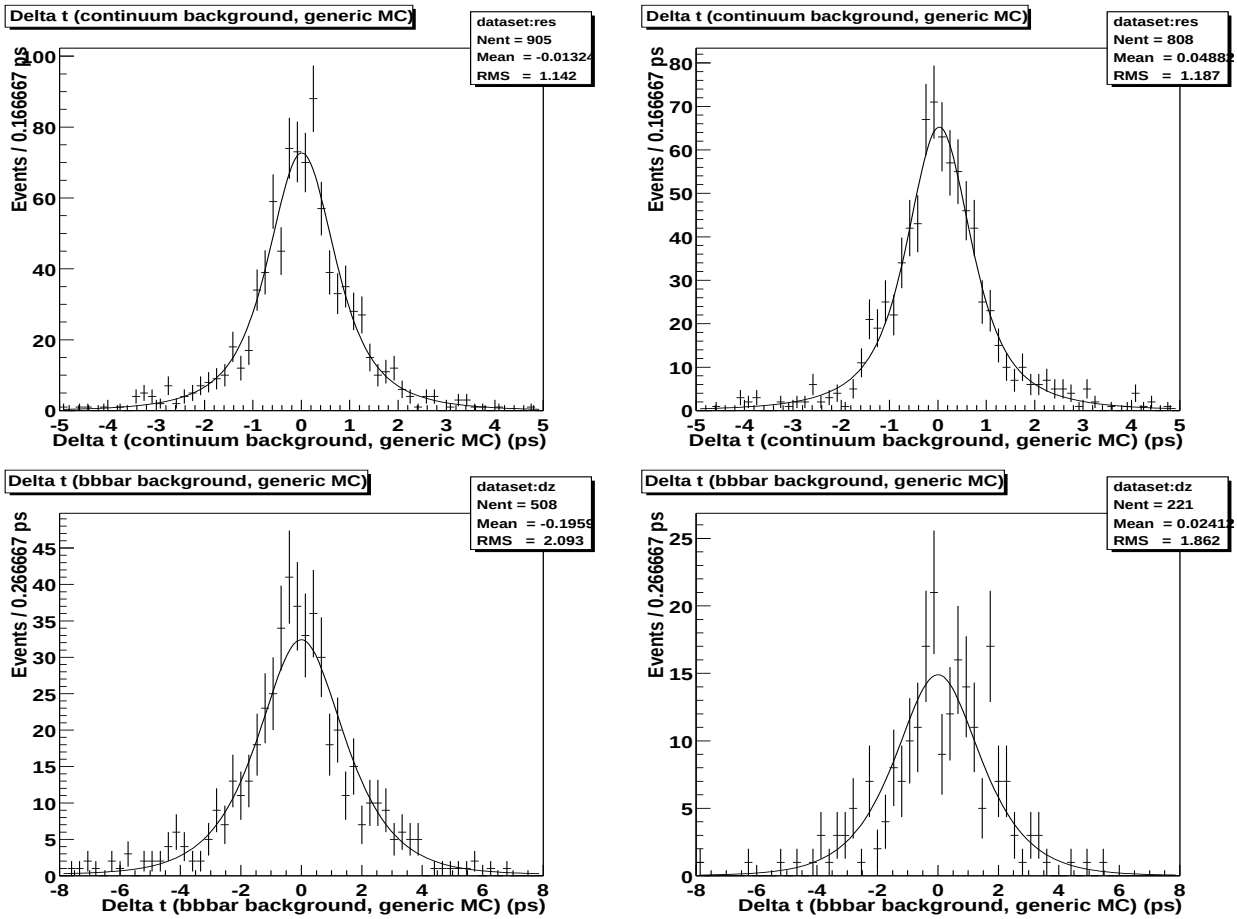

Figure 23: Δt distributions for background from continuum events (top) and $b\overline{b}$ events in the sideband region (bottom) obtained from generic Monte Carlo. Left: B^0, right: B^+.

To estimate the impact of the different compositions of the combinatorial background in the sideband and the signal region on the fitted B lifetimes, we generate Toy Monte Carlo samples with different background Δt distributions for events with $m_{\rm ES} < 5.27$ GeV and events with $m_{\rm ES} > 5.27$ GeV, and we use the nominal fitting procedure to extract the lifetime. The generated background Δt distributions are a sum of the two functions that we use to model the Δt distributions for background from continuum and $b\overline{b}$ generic Monte Carlo. The values of the parameters are those from the fit to generic Monte Carlo events listed in table 20. To generate sideband events, we set the fraction of the "δ contribution" to the fraction of continuum events in the Monte Carlo sideband, and to generate background events in the signal region, we set this fraction to the fraction of Monte Carlo continuum events in the signal region (table 19). The fitted B^0 (B^+) lifetime is overestimated by 0.0043 ± 0.0012 (Toy MC stat) ps (0.0090 ± 0.0011 (Toy MC stat) ps). We correct our measurements for this bias and assign the size of the correction as systematic uncertainty.

$\underline{B^0}$**:**

	continuum contribution in generic Monte Carlo	$b\overline{b}$ contribution in generic Monte Carlo
Two gaussian resolution function:		
f	0.91 ± 0.04	
s_1	1.17 ± 0.05	
b_1	0.009 ± 0.028 ps	
s_2	2.83 ± 0.43	
b_2	0.084 ± 0.236 ps	
Outlier fraction	$0.25 \pm 0.24\,\%$	
τ		1.00 ± 0.13 ps
Scale factor		1.39 ± 0.19
Outlier fraction		$0.52 \pm 0.18\,\%$
fraction of "flying contribution"	$33.6 \pm 1.7\,\%$ ($b\overline{b}$ fraction from table 19)	

$\underline{B^+}$**:**

	continuum contribution in generic Monte Carlo	$b\overline{b}$ contribution in generic Monte Carlo
Two gaussian resolution function:		
f	0.87 ± 0.04	
s_1	1.14 ± 0.05	
b_1	0.026 ± 0.029 ps	
s_2	3.16 ± 0.41	
b_2	0.034 ± 0.222 ps	
Outlier fraction	$0.97 \pm 0.51\,\%$	
τ		0.91 ± 0.14 ps
Scale factor		1.64 ± 0.25
Outlier fraction		$0.97 \pm 1.04\,\%$
fraction of "flying contribution"	$19.0 \pm 1.4\,\%$ ($b\overline{b}$ fraction from table 19)	

Table 20: Results of fits to the Δt distributions of combinatorial background in generic Monte Carlo.

The lifetime fit treats peaking background like signal. To a good approximation, peaking background from the "correct" B species behaves like signal (see section 4), and peaking background from the other B species behaves like signal with the lifetime of the other species. Our "B^0 signal" contains a B^+ contamination at the level of 1 % (see section 4), which has a lifetime that is roughly 6.2 % higher than the B^0 lifetime [1]. We expect the mean life of the contaminated B^0 sample to be $\simeq 1\,\% \cdot 6.2\,\% = 0.06\,\%$ higher than the B^0 lifetime. The "B^+ signal" contains a B^0 contamination at the 2 % level, and we expect its mean life to be $\simeq 2\,\% \cdot 5.8\,\% = 0.12\,\%$ lower than the B^+ lifetime. We correct our measurements for this bias and assign the size of the correction as systematic uncertainty. We assign an additional systematic uncertainty to account for a possible small deviation of the lifetime of peaking background from the lifetime of the B species that it is due to. Using high statistics Monte Carlo, the lifetime of peaking background from misreconstructed B^+ events in the sample of fully reconstructed B^0 events is tested to be consistent with the B^+ lifetime at the 7.8 % level [40]. We assign a systematic uncertainty of $1\,\% \cdot 7.8\,\%$ on the measured B^0 lifetime due to the uncertainty on the lifetime of peaking background from B^+ events, and a systematic uncertainty of $2\,\% \cdot 7.8\,\%$ on the measured B^0 lifetime due to the uncertainty on the lifetime of peaking background from B^0 events. The sum in quadrature of the three contributions to the systematic uncertainty due to the presence of peaking backgrounds in the B^0 sample is 0.0028 ps. We assign a systematic uncertainty of $2\,\% \cdot 7.8\,\%$ on the measured B^+ lifetime due to the uncertainty on the lifetime of peaking background from B^0 events, and a systematic uncertainty of $4\,\% \cdot 7.8\,\%$ on the measured B^+ lifetime due to the uncertainty on the lifetime of peaking background from B^+ events. The sum in quadrature of the three contributions to the systematic uncertainty due to the presence of peaking backgrounds in the B^+ sample is 0.0061 ps.

The sum in quadrature of the systematic uncertainties related to both combinatorial and peaking background is 0.0051 ps (0.0109 ps) for B^0 (B^+). It is listed as "background modelling" in table 21.

9.10 Monte Carlo test of fitting procedure

We perform a Toy Monte Carlo study to check the full fitting procedure used to extract the B lifetimes for any biases due to numerical limitations, fit parameters being close to a limit, and the cut on $|\Delta z|$. We generate 1200 Toy Monte Carlo samples using the result of the fit to the data (see section 8.1) as input. Only the input values for the two B lifetimes are taken from [1]. Figure 24 shows the distribution of the fitted values for the two B lifetimes and the corresponding pulls. The B^0 (B^+) lifetime is biased by 0.0024 ± 0.0009 ps (0.0032 ± 0.0009 ps) towards lower values. We correct our measurements for this bias. The correction is small compared to the systematic uncertainties from the validation studies on full Monte Carlo (see section 9.1), and we do not assign an additional systematic error. The width of the pull distributions is compatible with one, which indicates that the statistical error is reasonably well estimated.

9.11 Total systematic uncertainty

A summary of all systematic errors as well as their sum (in quadrature) is given in table 21.

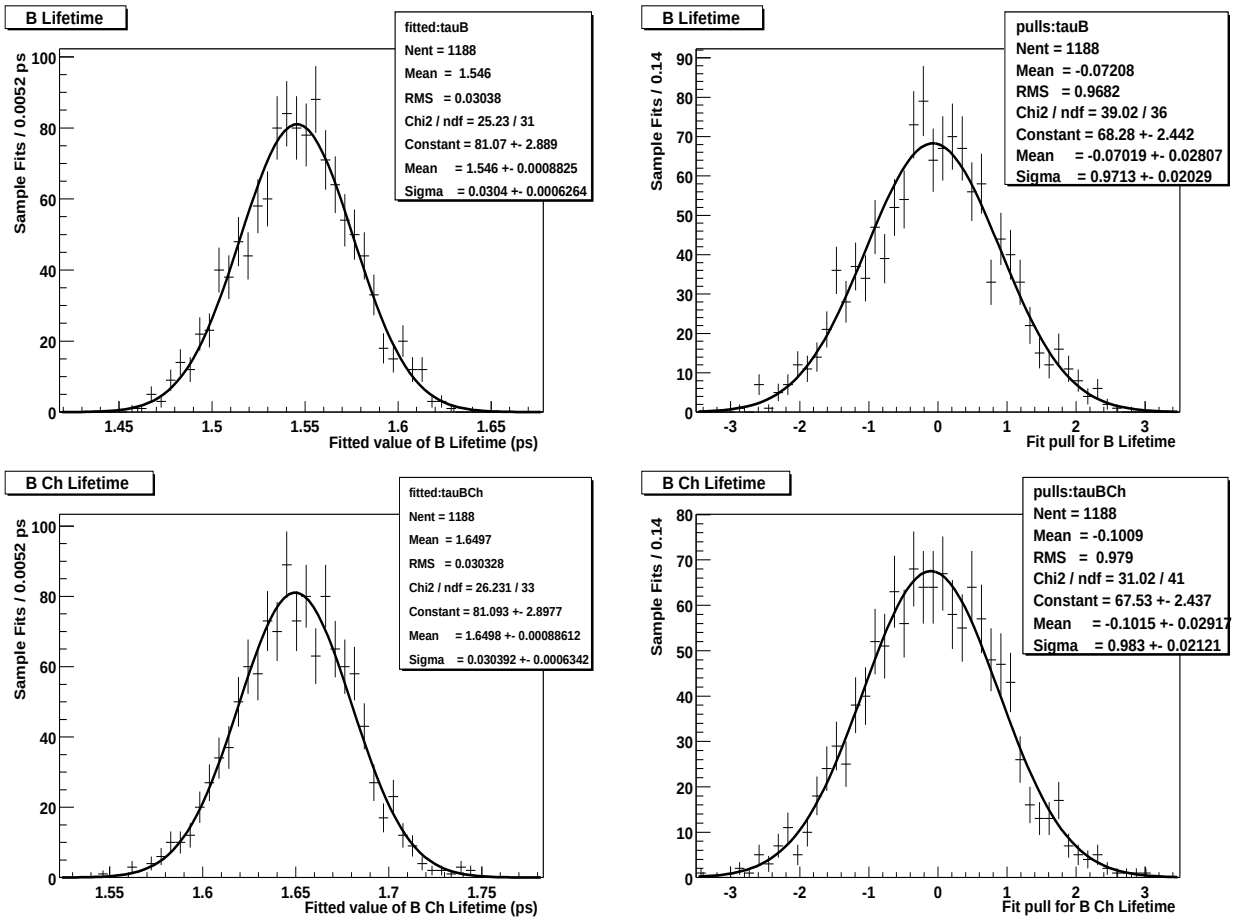

Figure 24: Results from Toy Monte Carlo test of the combined fit: distribution of fitted value of the lifetime (left) and the corresponding pull (right) for neutral (top) and charged (bottom) Bs.

Systematic effect	uncertainty on $\tau(B^0)$ (ps)	uncertainty on $\tau(B^+)$ (ps)
MC statistics	0.0087	0.0065
Parameterisation of resolution function	0.0075	0.0039
One single resolution function	0.0040	0.0052
Beam spot	0.0020	0.0020
Δt outliers	0.0114	0.0114
Residual alignment effects	0.0077	0.0077
z scale	0.0079	0.0084
Boost	0.0059	0.0063
Signal probability	0.0025	0.0029
Background modelling	0.0051	0.0109
Total in quadrature	0.0217	0.0227

Table 21: Summary of the systematic errors on the individual lifetimes.

10 Lifetime ratio

We replace the two lifetimes in our fit by the B^0 lifetime and the ratio $r = \frac{\tau(B^+)}{\tau(B^0)}$.

10.1 Fit result

Parameters:

1-2: centre and width of outlier gaussian (B^0)
3: B^0 lifetime
4-6: resolution function
7: $f_{\mathrm{out,S}}$ (in per mil), B^0 sample
8-9 and 18-20: B^0 candidate mass spectrum
10-17: background, B^0 sample
21-22: centre and width of outlier gaussian (B^+)
23: lifetime ratio
24: $f_{\mathrm{out,S}}$ (in per mil), B^+ sample
25-26 and 35-37: B^+ candidate mass spectrum
27-34: background, B^+ sample

```
**********
**   17 **HESSE        6750
**********
COVARIANCE MATRIX CALCULATED SUCCESSFULLY
FCN=-3949.81 FROM HESSE     STATUS=OK            248 CALLS        1056 TOTAL
                     EDM=0.000787653    STRATEGY= 1      ERROR MATRIX ACCURATE
 EXT PARAMETER                                   INTERNAL      INTERNAL
 NO.   NAME      VALUE            ERROR       STEP SIZE       VALUE
  1  zentrum      0.00000e+00   constant
  2  breite       1.00000e+01   constant
  3  tauB         1.56062e+00   3.19650e-02   1.44310e-04   1.56062e+00
  4  sigma        1.20709e+00   6.98322e-02   4.38544e-04   1.20709e+00
  5  frac         6.90643e-01   7.36984e-02   5.51620e-04   3.91187e-01
  6  tau          1.03426e+00   2.44313e-01   5.36485e-04  -3.15710e-01
  7  outFrac      1.88413e+00   2.28320e+00   8.20730e-05  -1.48396e+00
  8  bmass        5.28019e+00     fixed
  9  bresn        2.73518e-03     fixed
 10  bOutBckg     0.00000e+00   constant
 11  sOutBckg     1.00000e+01   constant
 12  tauBckg      1.17006e+00   8.21624e-02   3.78077e-04   1.17006e+00
 13  sigmaBckg    1.34692e+00   3.71870e-02   1.98347e-04   1.34692e+00
 14  frBckg       8.94441e-01   2.21303e-02   1.16427e-04   8.94441e-01
 15  tauRBckg     1.74240e+00   2.63501e-01   1.37446e-03   1.74240e+00
 16  fLifeBckg    3.67766e-01   4.24375e-02   1.60291e-04   3.67766e-01
 17  fOutBckg     7.24569e+00   2.22554e+00   2.01302e-04  -1.40035e+00
 18  endpt        5.29078e+00     fixed
 19  c           -3.25892e+01     fixed
 20  f            4.81471e-01     fixed
 21  zentrumCh    0.00000e+00   constant
 22  breiteCh     1.00000e+01   constant
 23  ratio        1.07360e+00   2.56017e-02   1.35846e-04   1.07360e+00
 24  outFracCh    1.98518e+00   2.55190e+00   8.74574e-05  -1.48166e+00
 25  bmassCh      5.27992e+00     fixed
 26  bresnCh      2.57999e-03     fixed
 27  bOutBckgCh   0.00000e+00   constant
 28  sOutBckgCh   1.00000e+01   constant
 29  tauBckgCh    1.18210e+00   1.13271e-01   4.74187e-04   1.18210e+00
 30  sigmaBckgCh   1.38134e+00   3.88673e-02   2.18875e-04   1.38134e+00
 31  frBckgCh     9.14814e-01   3.18849e-02   1.57934e-04   9.14814e-01
 32  tauRBckgCh   1.41515e+00   3.75792e-01   1.82212e-03   1.41515e+00
 33  fLifeBckgCh   3.14212e-01   4.48950e-02   1.70287e-04   3.14212e-01
 34  fOutBckgCh   5.59365e+00   2.54699e+00   2.44545e-04  -1.42108e+00
 35  endptCh      5.29039e+00     fixed
 36  cCh         -3.29734e+01     fixed
 37  fCh          5.72333e-01     fixed
                           ERR DEF= 0.5
EXTERNAL ERROR MATRIX.    NDIM=  37    NPAR= 19    ERR DEF=0.5
 [covariance matrix omitted]

PARAMETER  CORRELATION COEFFICIENTS
      NO.  GLOBAL      3      4      5      6      7     12     13     14     15     16     17     23     24     29     30     31
       3  0.85415   1.000 -0.406 -0.179 -0.208 -0.376 -0.052  0.025  0.003  0.008 -0.003  0.020 -0.645 -0.070 -0.005  0.019  0.008
       4  0.69029  -0.406  1.000 -0.217 -0.313  0.125 -0.001 -0.069 -0.002  0.009  0.017 -0.005  0.091  0.103  0.003 -0.045 -0.004
```

```
  5  0.91822  -0.179 -0.217  1.000  0.911 -0.054  0.010  0.005 -0.059 -0.056 -0.008  0.008  0.001  0.019  0.007  0.002 -0.045
  6  0.93325  -0.208 -0.313  0.911  1.000 -0.061  0.014  0.013 -0.038 -0.056 -0.008  0.009 -0.005  0.030  0.008  0.009 -0.029
  7  0.43418  -0.376  0.125 -0.054 -0.061  1.000  0.049 -0.000  0.003  0.005 -0.012 -0.128  0.295  0.012  0.000 -0.005  0.001
 12  0.84779  -0.052 -0.001  0.010  0.014  0.049  1.000  0.317 -0.101 -0.236 -0.731 -0.333  0.040  0.001  0.000 -0.000 -0.000
 13  0.78904   0.025 -0.069  0.005  0.013 -0.000  0.317  1.000  0.223  0.144 -0.678 -0.105 -0.002 -0.007 -0.000  0.003  0.001
 14  0.79548   0.003 -0.002 -0.059 -0.038  0.003 -0.101  0.223  1.000  0.721  0.077 -0.088  0.003 -0.000 -0.000  0.001  0.004
 15  0.79946   0.008  0.009 -0.056 -0.056  0.005 -0.236  0.144  0.721  1.000  0.042 -0.155  0.004 -0.002 -0.000 -0.000  0.002
 16  0.90047  -0.003  0.017 -0.008 -0.008 -0.012 -0.731 -0.678  0.077  0.042  1.000  0.187 -0.001  0.002  0.000 -0.001  0.000
 17  0.46798   0.020 -0.005  0.008  0.009 -0.128 -0.333 -0.105 -0.088 -0.155  0.187  1.000 -0.018  0.000  0.000  0.000 -0.000
 23  0.79141  -0.645  0.091  0.001 -0.005  0.295  0.040 -0.002  0.003  0.004 -0.001 -0.018  1.000 -0.305 -0.028 -0.008 -0.002
 24  0.48068  -0.070  0.103  0.019  0.030  0.012  0.001 -0.007 -0.000 -0.002  0.002  0.000 -0.305  1.000  0.044  0.006  0.000
 29  0.87601  -0.005  0.003  0.007  0.008  0.000  0.000 -0.000 -0.000 -0.000  0.000  0.000 -0.028  0.044  1.000  0.339 -0.149
 30  0.76115   0.019 -0.045  0.002  0.009 -0.005 -0.000  0.003  0.001 -0.000 -0.001  0.000 -0.008  0.006  0.339  1.000  0.225
 31  0.82138   0.008 -0.004 -0.045 -0.029  0.001 -0.000  0.001  0.004  0.002  0.000 -0.000 -0.002  0.000 -0.149  0.225  1.000
 32  0.82956   0.011 -0.000 -0.035 -0.032  0.001 -0.000  0.000  0.002  0.002  0.000 -0.000  0.001 -0.002 -0.263  0.120  0.763
               1.000  0.036 -0.013
 33  0.89953  -0.001  0.004 -0.005 -0.005  0.001 -0.000 -0.000  0.000  0.000  0.000 -0.000  0.003 -0.017 -0.759 -0.651  0.068
               0.036  1.000  0.312
 34  0.56507  -0.000  0.000  0.000  0.000  0.000 -0.000 -0.000 -0.000 -0.000  0.000 -0.000  0.014 -0.077 -0.506 -0.155 -0.016
              -0.013  0.312  1.000


**********
**   17 **MINOS        6750
**********
FCN=-3949.81 FROM MINOS     STATUS=SUCCESSFUL   8359 CALLS        9167 TOTAL
                    EDM=0.000786217    STRATEGY= 1      ERROR MATRIX ACCURATE
 EXT PARAMETER                PARABOLIC          MINOS ERRORS
 NO.   NAME      VALUE            ERROR      NEGATIVE      POSITIVE
  1  zentrum      0.00000e+00   constant
  2  breite       1.00000e+01   constant
  3  tauB         1.56062e+00   3.19500e-02  -3.22004e-02   3.17874e-02
  4  sigma        1.20709e+00   6.97598e-02  -6.99739e-02   7.00091e-02
  5  frac         6.90643e-01   7.35562e-02  -9.41106e-02   6.33583e-02
  6  tau          1.03426e+00   2.43789e-01  -2.48117e-01   2.51448e-01
  7  outFrac      1.88413e+00   2.28497e+00   at limit      2.55616e+00
  8  bmass        5.28019e+00     fixed
  9  bresn        2.73518e-03     fixed
 10  bOutBckg     0.00000e+00   constant
 11  sOutBckg     1.00000e+01   constant
 12  tauBckg      1.17006e+00   8.23075e-02  -7.75004e-02   8.76743e-02
 13  sigmaBckg    1.34692e+00   3.71354e-02  -3.68095e-02   3.76250e-02
 14  frBckg       8.94441e-01   2.21335e-02  -2.33800e-02   2.10566e-02
 15  tauRBckg     1.74240e+00   2.63202e-01  -2.50670e-01   2.83174e-01
 16  fLifeBckg    3.67766e-01   4.24761e-02  -4.18453e-02   4.29420e-02
 17  fOutBckg     7.24569e+00   2.22493e+00  -2.06325e+00   2.38589e+00
 18  endpt        5.29078e+00     fixed
 19  c           -3.25892e+01     fixed
 20  f            4.81471e-01     fixed
 21  zentrumCh    0.00000e+00   constant
 22  breiteCh     1.00000e+01   constant
 23  ratio        1.07360e+00   2.56046e-02  -2.50757e-02   2.61930e-02
 24  outFracCh    1.98518e+00   2.55515e+00   at limit      2.78684e+00
 25  bmassCh      5.27992e+00     fixed
 26  bresnCh      2.57999e-03     fixed
 27  bOutBckgCh   0.00000e+00   constant
 28  sOutBckgCh   1.00000e+01   constant
 29  tauBckgCh    1.18210e+00   1.13408e-01  -1.08091e-01   1.18779e-01
 30  sigmaBckgCh   1.38134e+00   3.88306e-02  -3.88544e-02   3.89413e-02
 31  frBckgCh     9.14814e-01   3.19024e-02  -3.69691e-02   2.83518e-02
 32  tauRBckgCh   1.41515e+00   3.75431e-01  -3.59322e-01   4.11929e-01
 33  fLifeBckgCh   3.14212e-01   4.49511e-02  -4.27538e-02   4.70799e-02
 34  fOutBckgCh   5.59365e+00   2.54513e+00  -2.29556e+00   2.78974e+00
 35  endptCh      5.29039e+00     fixed
 36  cCh         -3.29734e+01     fixed
 37  fCh          5.72333e-01     fixed
                             ERR DEF= 0.5
```

Summary:

$\tau(B^0) = 1.561 \pm 0.032$ ps
$r = 1.074 \pm 0.026$

10.2 Systematic uncertainties

We repeat the studies of systematic uncertainties described in section 9 for the new set of variables.

10.2.1 Sample selection

We repeat the combined fit to the high statistics signal Monte Carlo sample described in section 9.1, and fit for the lifetime ratio. The result $r = 1.0697 \pm 0.0063$ is consistent with the generated value $r = 1.0678$. We assign 0.0063 as systematic uncertainty on our measurements on data.

10.2.2 Parameterisation of the resolution function

We propagate the bias on the two individual lifetimes estimated in section 9.2 on the lifetime ratio. This bias leads to an underestimation of the lifetime ratio by $\frac{1.6530 \text{ ps}}{1.5480 \text{ ps}} - \frac{1.6530 \text{ ps}+0.0039 \text{ ps}}{1.5480 \text{ ps}+0.0075 \text{ ps}} = 0.0026$. We correct our measurement of the lifetime ratio for this bias and assign the size of the correction as systematic uncertainty.

10.2.3 Identical resolution function

We propagate the bias on the two individual lifetimes due to the approximation of equal resolution functions for charged and neutral Bs (see section 9.3) on the lifetime ratio. This bias leads to an underestimation of the lifetime ratio by $\frac{1.6530 \text{ ps}}{1.5480 \text{ ps}} - \frac{1.6530 \text{ ps}-0.0052 \text{ ps}}{1.5480 \text{ ps}+0.0040 \text{ ps}} = 0.0061$. We correct our measurement of the lifetime ratio for this bias and assign the size of the correction as systematic uncertainty.

10.2.4 Beam spot

Any systematic bias in the beam spot determination affects the Δt resolution functions for neutral and charged Bs in a similar way. Any residual effects that cannot be absorbed by our parameterisation of the resolution function cancel to a good approximation when the lifetime ratio is calculated. At the present level of precision we neglect any residual effects.

10.2.5 Δt outliers

The effect of Δt outliers on the fitted result for r is small if the properties of the outliers in the B^0 and the B^+ sample are similar, i.e. if the fractions and the Δt distributions of outliers are close. The fraction of outliers in the B^0 sample and the fraction of outliers in the B^+ sample are independent free parameters in the lifetime fit (see section 6.3) and the uncertainty due to a possible difference between the two fractions is included in the statistical error on r.

Given the results of section 9.5, we neglect the effects of a possible difference in the mean values of the two outlier Δt distributions. To estimate the uncertainty due to a possible difference in the width of the two outlier Δt distributions, we propagate the biases listed in table 16 on the lifetime ratio. Table 22 shows the bias on the ratio for different combinations of values for the two widths. From fits to the outlier Δt residual distributions in signal Monte Carlo, where outliers have been identified using a cut on the per-event Δt pull (see section 5.3.3), we obtain 7.2 ± 0.9 ps (B^0) and 7.6 ± 1.1 ps (B^+). The two widths agree at the 2 ps level, and we assign 0.0045 (from table 22) as systematic uncertainty.

Width (outliers B^0)	Width (outliers B^+)	Frac = 0.2 %	Frac = 0.35 %	Frac = 0.5 %
15 ps	12 ps	+0.0021	+0.0018	+0.0043
12 ps	15 ps	−0.0019	−0.0014	−0.0037
12 ps	10 ps	+0.0008	+0.0026	+0.0021
10 ps	8 ps	+0.0013	+0.0038	+0.0045
8 ps	6 ps	+0.0006	+0.0009	+0.0025
6 ps	4 ps	−0.0018	−0.0033	−0.0045

Table 22: Shift of the fitted lifetime ratio ($r(\text{fitted}) - r(\text{generated})$) for different outlier Δt distributions used at generation time.

10.2.6 Detector geometry and alignment

The z scale uncertainties cancel to a good approximation when the lifetime ratio is calculated. Any distortions due to imperfections in the detector alignment affect the Δt resolution functions for neutral and charged Bs in a similar way. Any residual effects that cannot be absorbed by our parameterisation of the resolution function cancel to a good approximation when the lifetime ratio is calculated. At the present level of precision we neglect any residual effects.

10.2.7 Approximate Δt calculation and uncertainty on the average boost

As discussed in section 9.7, the approximations involved in the Δz to Δt conversion lead to an additional smearing that is at least partially absorbed by the Δt resolution function. Any residual effects are included in the resolution function systematics discussed in section 10.2.2. The uncertainties due to the finite precision of the boost determination cancel to a good approximation when the lifetime ratio is calculated. At the present level of precision we neglect any residual effects.

10.2.8 Signal probability

We repeat the variation study described in section 9.8, fitting for the lifetime ratio. Varying the fraction of signal events in the B^0 (B^+) sample changes the lifetime ratio by 0.0012 (0.0012); varying the value of the Argus shape parameter changes the lifetime ratio by 0.0013 (0.0014). The variation of any other parameter changes the lifetime ratio by less than 0.0005. We assign the sum in quadrature of these four contributions as systematic uncertainty due to the uncertainty on the signal probability.

10.2.9 Background modelling

We propagate the bias on the two individual lifetimes due to the different compositions of the combinatorial background in the $m_{\rm ES}$ sideband and the signal region (see section 9.9) on the lifetime ratio. This bias leads to an overestimation of the lifetime ratio by $\frac{1.6530 \text{ ps}+0.0090 \text{ ps}}{1.5480 \text{ ps}+0.0043 \text{ ps}} -$

$\frac{1.6530\text{ ps}}{1.5480\text{ ps}} = 0.0028$. We correct our measurement of the lifetime ratio for this bias and assign the size of the correction as systematic uncertainty.

The differences in the composition of the combinatorial background in the $m_{\rm ES}$ sideband and the signal region bias the measurements of both $\tau(B^0)$ and $\tau(B^+)$ in the same direction: the combinatorial background in the signal region is enriched in $b\overline{b}$ events and has a broader Δt distribution than the combinatorial background in the sideband region. This leads to an overestimation of both lifetimes, and the effects partially cancel when the lifetime ratio is calculated. The presence of peaking backgrounds from the "wrong" B species (see section 4.3) "pulls both measured lifetimes closer to each other", and the effects add up when the ratio is calculated. This leads to an underestimation of the lifetime ratio by $0.06\,\% + 0.12\,\% = 0.0018$. We correct our measurement of the ratio for this bias and assign the size of the correction as systematic uncertainty. We propagate the two contributions from the uncertainty on the lifetimes of peaking backgrounds to the uncertainties on each of the two individual lifetimes on the ratio. The sum in quadrature of the five contributions to the uncertainty on the ratio due to the presence of peaking backgrounds is 0.0044.

The total systematic uncertainty on the lifetime ratio due to the presence of both combinatorial and peaking backgrounds is $\sqrt{0.0028^2 + 0.0044^2} = 0.0052$.

10.2.10 Monte Carlo test of fitting procedure

We repeat the Toy Monte Carlo study described in section 9.10, fitting for the lifetime ratio. The distribution of fitted values of the lifetime ratio as well as the corresponding pull are shown in figure 25. The small biases on the individual lifetimes discussed in section 9.10 cancel to a good approximation and at the present level of accuracy we neglect any residual effects.

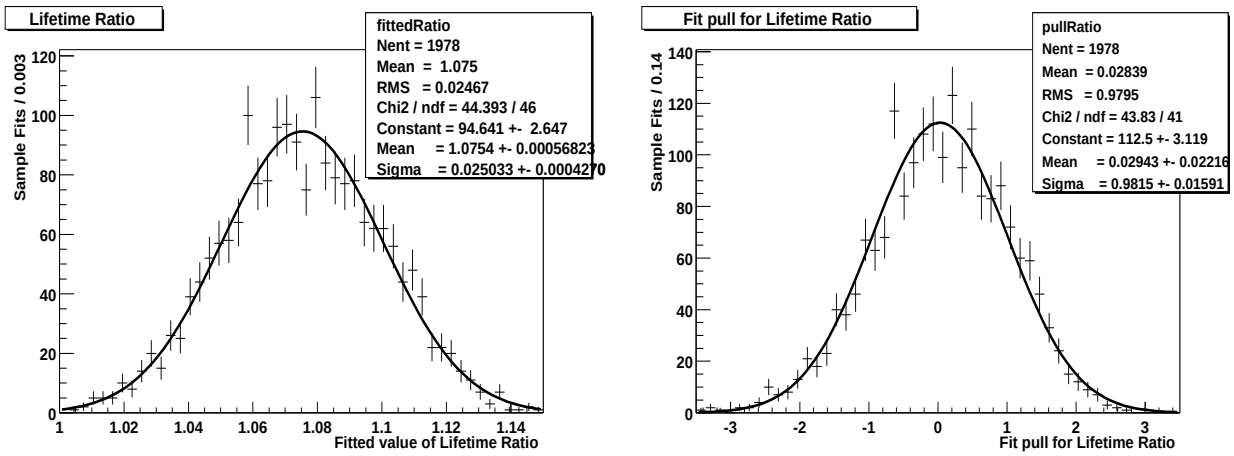

Figure 25: Results from Toy Monte Carlo test of the combined fit: distribution of fitted value of the lifetime ratio (left) and the corresponding pull (right). The generated value of the lifetime ratio is 1.07380 .

10.2.11 Total systematic uncertainty

A summary of all systematic errors as well as their sum (in quadrature) is given in table 23.

Systematic effect	uncertainty on r	comment
MC statistics	0.0063	
Parameterisation of resolution function	0.0026	
One single resolution function	0.0061	
Beam spot	-	cancels
Δt outliers	0.0045	
Residual alignment effects	-	cancels
z scale	-	cancels
Boost	-	cancels
Signal probability	0.0026	
Background modelling	0.0052	
Total in quadrature	0.0117	

Table 23: Summary of the systematic uncertainties on the lifetime ratio r.

11 Conclusion

We add up all uncertainties and apply the corrections discussed in section 9. The final result reads

$$\tau(B^0) = 1.546 \pm 0.032 \text{ (stat)} \pm 0.022 \text{ (syst) ps}$$
$$\tau(B^+) = 1.673 \pm 0.032 \text{ (stat)} \pm 0.023 \text{ (syst) ps}$$
$$\frac{\tau(B^+)}{\tau(B^0)} = 1.082 \pm 0.026 \text{ (stat)} \pm 0.012 \text{ (syst)},$$

where the first error is statistical (see the discussion in section 9.2) and the second one is sytematic.

12 Acknowledgements

It is a pleasure to thank Jochen Schieck, Andrei Gritsan, Bill Dunwoodie, Carsten Hast, Jean-Pierre Lees, Patrick Robbe, Eric Charles, Alexis Pompili, Gabriele Simi and Eugenio Paoloni for stimulating discussions about tracking and alignment issues, as well as Ben Brau, Patrick Robbe and Julian von Wimmersperg-Toeller for their help in the B sample preparation. We are grateful for the countless useful suggestions from habitués of the Breco (convenors: Vivek Sharma and Yury Kolomensky), Vertexing and Lifetime/Mixing (convenors: David Kirkby and Gerhard Raven) AWG meetings and from the review committee (Sören Prell, Doug Roberts, Gérard Bonneaud and Alessandro Calcaterra).

References

[1] Particle Data Group, D.E. Groom *et al.*, "Review of particle physics", Eur. Phys. J. C **15**, 1 (2000).

[2] I. I. Bigi, "Lifetimes of heavy flavor hadrons: whence and whither ?", Nuovo Cim. **109 A**, 713 (1996).

[3] M. Neubert, C. T. Sachrajda, "Spectator effects in inclusive decays of beauty hadrons", Nucl. Phys. B **483**, 339 (1997).

[4] J. Chauveau *et al.*, "B lifetime measurement using exclusively reconstructed hadronic B decays", *BABAR* analysis document 37 (2000).

[5] *BABAR* collaboration, B. Aubert *et al.*, "A measurement of the charged and neutral B meson lifetimes using fully reconstructed decays", *BABAR*-CONF-00/07 and `hep-ex/0008060` (2000).

[6] R. Kerth *et al.*, "The *BABAR* coordinate system and units", *BABAR* note 230 (1995).

[7] D. Kirkby, "Generator-level studies for $B\overline{B}$ mixing", http://www.slac.stanford.edu/∼davidk/BBMix/GenStudy/ (1999).

[8] P. F. Harrison and H. R. Quinn, eds., "The *BABAR* physics book", SLAC-R-405 (1998), section 11.3.

[9] J. Blouw, A. Soffer and S. Dong, "Measuring the PEP-II boost", *BABAR* analysis document 14 (2000).

[10] Vertexing and Composition Tools group, "The *BABAR* vertexing", *BABAR* analysis document 102 (2000).

[11] *BABAR* collaboration, B. Aubert *et al.*, "The first year of the *BABAR* experiment at PEP-II", *BABAR*-CONF-00/17 and `hep-ex/0012042` (2000).

[12] E. Robutti, "*BABAR* datasets", http://www.slac.stanford.edu/BFROOT/www/Physics/BaBarData/GoodRuns/dataSets.html (2000).

[13] C. Touramanis, "Luminosity", February Collaboration Meeting, Physics analysis plenary session (2001).

[14] C. Hearty, "Measurement of the number of $\Upsilon(4S)$ mesons produced in Run1 (B Counting) ", *BABAR* analysis document 134 (2001).

[15] Breco AWG, "Exclusive reconstruction of hadronic B decays to open charm", *BABAR* analysis document 150 (2001).

[16] Charmonium AWG, "Measurement of exclusive charmonium branching ratios using data from BaBar's first run", *BABAR* analysis document 113 (2001).

[17] ARGUS collaboration, H. Albrecht *et al.*, "Exclusive hadronic decays of B mesons", Z. Phys. **C48**, 543 (1990).

[18] P. Robbe, "Breco modes - Background studies", presentation given at the Breco meeting on Nov 16^{th} (2000).

[19] R. Faccini and F. Martínez-Vidal, "Vertexing/kinematic fitting user's guide", http://www.slac.stanford.edu/BFROOT/www/Physics/Tools/Vertex/VtxGuide (2000).

[20] C. de la Vaissière, H. Briand and N. Regnault, "Lifetimes with full B reconstruction", *BABAR* note 436 (1998).

[21] F. Martínez-Vidal, "VtxTagBtaSelFit: a vertex tag reconstruction tool user's guide", http://www.slac.stanford.edu/BFROOT/www/Physics/Tools/Vertex/VtxGuide/VtxTagBtaSelFit.html (2000).

[22] T. Skwarnicki, "A study of the radiative cascade transitions between upsilon-prime and upsilon resonances", DESY F31-86-02 (thesis, unpublished) (1986).

[23] J. Stark, "B^0/B^+ lifetimes with fully reconstructed hadronic B decays and the Δz resolution function", April Physics Week (2000).

[24] Vertexing and Composition Tools group, "Vertexing performances and systematic checks with fully reconstructed B events", *BABAR* analysis document 130 (2001).

[25] J. Back *et al.*, "A user's guide to the `RooFitTools` package for unbinned maximum likelihood fitting", *BABAR* analysis document 18 (2001).

[26] F. James, "Minuit. Function minimization and error analysis", CERN program library long writeup D506 (1994).

[27] Vertexing and Composition Tools group, "Vertexing control samples", *BABAR* analysis document 183 (2001).

[28] M.-H. Schune, "Re: DECAY file updates for SP4: χ_d for signal $D^* l\nu$??", Physics analysis hypernews 1058/1 (2001), and replies.

[29] G. Raven, "Exclusive B^0 cocktail MC decay file updated, wrong χ_d in SP3", $B^0/\overline{B^0}$ mixing analysis hypernews 228 (2001).

[30] C. Cheng *et al.*, "Beam spot determination and use in *BABAR*", *BABAR* analysis document 13 (2000).

[31] C. Cheng, "Beam spot variation within a run (14459)", Sin2beta hypernews 210 (2001).

[32] A. V. Gritsan, "SVT local alignment systematics", Physics analysis hypernews 1023 (2001).

[33] A. V. Gritsan, "SVT local alignment systematics for Run1 data", February Collaboration Meeting, Vertexing parallel session (2001).

[34] G. Raven, private communication (2001).

[35] *BABAR* collaboration, D. Boutigny *et al.*, "Technical design report", SLAC-R-95-457 (1995).

[36] W. Dunwoodie *et al.*, "Study of material interactions with gamma conversions and protons", *BABAR* analysis document 106 (2001).

[37] A. Ryd *et al.*, "EvtGen. A Monte Carlo generator for B-physics", included in the CVS repository of the package (2000).

[38] Presentations given at the Forum meeting on May 16^{th} (2000).

[39] N. L. Johnson, "Systems of frequency curves generated by methods of translation", Biometrika **36**, 149 (1949). The definition can also be found in [25].

[40] Ben Brau, private communication, to be incorporated into [15] (2001).